Article

# Structure and Reactivity of Bis(silyl) Dihydride Complexes (PMe)Ru(SiR)(H): Model Compounds and Real Intermediates in a Dehydrogenative C–Si Bond Forming Reaction

Vladimir K. Dioumaev, Bok R. Yoo, Leo J. Procopio, Patrick J. Carroll, and Donald H. Berry

*J. Am. Chem. Soc.*, **2003**, 125 (29), 8936-8948• DOI: 10.1021/ja035916v • Publication Date (Web): 25 June 2003



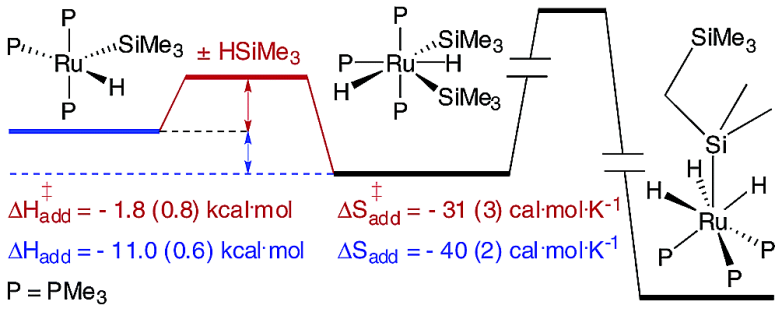


## More About This Article

Additional resources and features associated with this article are available within the HTML version:

- Supporting Information
- Links to the 5 articles that cite this article, as of the time of this article download
- Access to high resolution figures
- Links to articles and content related to this article
- Copyright permission to reproduce figures and/or text from this article

View the Full Text HTML

J|A|C|S
ARTICLES
Published on Web 06/25/2003

# Structure and Reactivity of Bis(silyl) Dihydride Complexes $(PMe_3)_3Ru(SiR_3)_2(H)_2$: Model Compounds and Real Intermediates in a Dehydrogenative C−Si Bond Forming Reaction

Vladimir K. Dioumaev, Bok R. Yoo, Leo J. Procopio, Patrick J. Carroll, and Donald H. Berry*

*Contribution from the Department of Chemistry and Laboratory for Research on the Structure of Matter, University of Pennsylvania, Philadelphia, Pennsylvania 19104-6323*

Received May 2, 2003; E-mail: dberry@sas.upenn.edu

***Abstract:*** A series of stable complexes, $(PMe_3)_3Ru(SiR_3)_2(H)_2$ ($(SiR_3)_2 = (SiH_2Ph)_2$, **3a**; $(SiHPh_2)_2$, **3b**; $(SiMe_2CH_2CH_2SiMe_2)$, **3c**), has been synthesized by the reaction of hydridosilanes with $(PMe_3)_3Ru(SiMe_3)H_3$ or $(PMe_3)_4Ru(SiMe_3)H$. Compounds **3a** and **3c** adopt overall pentagonal bipyramidal geometries in solution and the solid state, with phosphine and silyl ligands defining trigonal bipyramids and ruthenium hydrides arranged in the equatorial plane. Compound **3a** exhibits meridional phosphines, with both silyl ligands equatorial, whereas the constraints of the chelate in **3c** result in both axial and equatorial silyl environments and facial phosphines. Although there is no evidence for agostic Si−H interactions in **3a** and **3b**, the equatorial silyl group in **3c** is in close contact with one hydride (1.81(4) Å) and is moderately close to the other hydride (2.15(3) Å) in the solid state and solution ($\nu$(Ru···H···Si) = 1740 cm$^{-1}$ and $\nu$(RuH) = 1940 cm$^{-1}$). The analogous bis(silyl) dihydride, $(PMe_3)_3Ru(SiMe_3)_2(H)_2$ (**3d**), is not stable at room temperature, but can be generated in situ at low temperature from the 16e$^-$ complex $(PMe_3)_3Ru(SiMe_3)H$ (**1**) and $HSiMe_3$. Complexes **3b** and **3d** have been characterized by multinuclear, variable temperature NMR and appear to be isostructural with **3a**. All four complexes exhibit dynamic NMR spectra, but the slow exchange limit could not be observed for **3c.** Treatment of **1** with $HSiMe_3$ at room temperature leads to formation of $(PMe_3)_3Ru(SiMe_2CH_2SiMe_3)H_3$ (**4b**) via a CH functionalization process critical to catalytic dehydrocoupling of $HSiMe_3$ at higher temperatures. Closer inspection of this reaction between −110 and −10 °C by NMR reveals a plethora of silyl hydride phosphine complexes formed by ligand redistribution prior to CH activation. Above ca. 0 °C this mixture converts cleanly via silane dehydrogenation to the very stable tris(phosphine) trihydride carbosilyl complex **4b**. The structure of **4b** was determined crystallographically and exhibits a tetrahedral $P_3Si$ environment around the metal with the three hydrides adjacent to silicon and capping the $P_2Si$ faces. Although strong Si···HRu interactions are not indicated in the structure or by IR, the HSi distances (2.00(4) − 2.09(4) Å) and average coupling constant ($J_{SiH}$ = 25 Hz) suggest some degree of nonclassical SiH bonding in the $RuH_3Si$ moiety. The least hindered complex, **3a**, reacts with carbon monoxide principally via an $H_2$ elimination pathway to yield *mer*-$(PMe_3)_3(CO)Ru(SiH_2Ph)_2$, with SiH elimination as a minor process. However, only SiH elimination and formation of $(PMe_3)_3(CO)Ru(SiR_3)H$ is observed for **3b**−**d**. The most hindered bis(silyl) complex, **3d**, is extremely labile and even in the absence of CO undergoes SiH reductive elimination to generate the 16e$^-$ species **1** ($\Delta H_{SiH-elim}$ = 11.0 ± 0.6 kcal·mol$^{-1}$ and $\Delta S_{SiH-elim}$ = 40 ± 2 cal·mol$^{-1}$·K$^{-1}$; $\Delta H^{\ddagger}_{SiH-elim}$ = 9.2 ± 0.8 kcal·mol$^{-1}$ and $\Delta S^{\ddagger}_{SiH-elim}$ = 9 ± 3 cal·mol$^{-1}$·K$^{-1}$). The *minimum* barrier for the $H_2$ reductive elimination can be estimated, and is higher than that for silane elimination at temperatures above ca. −50 °C. The thermodynamic preferences for oxidative additions to **1** are dominated by entropy contributions and steric effects. Addition of $H_2$ is by far most favorable, whereas the relative aptitudes for intramolecular silyl CH activation and intermolecular SiH addition are strongly dependent on temperature ($\Delta H_{SiH-add}$ = −11.0 ± 0.6 kcal·mol$^{-1}$ and $\Delta S_{SiH-add}$ = −40 ± 2 cal·mol$^{-1}$·K$^{-1}$; $\Delta H_{\beta-CH-add}$ = −2.7 ± 0.3 kcal·mol$^{-1}$ and $\Delta S_{\beta-CH-add}$ = −6 ± 1 cal·mol$^{-1}$·K$^{-1}$). Kinetic preferences for oxidative additions to **1** − intermolecular SiH and intramolecular CH − have been also quantified: $\Delta H^{\ddagger}_{SiH-add}$ = −1.8 ± 0.8 kcal·mol$^{-1}$ and $\Delta S^{\ddagger}_{SiH-add}$ = −31 ± 3 cal·mol$^{-1}$·K$^{-1}$; $\Delta H^{\ddagger}_{\beta-CH-add}$ = 16.4 ± 0.6 kcal·mol$^{-1}$ and $\Delta S^{\ddagger}_{\beta-CH-add}$ = −13 ± 6 cal·mol$^{-1}$·K$^{-1}$. The relative enthalpies of activation are interpreted in terms of strong SiH $\sigma$-complex formation − and much weaker CH coordination − in the transition state for oxidative addition.

## Introduction

The dehydrogenative coupling of alkylsilanes to carbosilanes in the presence of ruthenium and rhodium complexes is an unusual example of catalytic functionalization of aliphatic C−H bonds.[1−4] In a recent report, we described direct observation of

(1) Procopio, L. J.; Berry, D. H. *J. Am. Chem. Soc.* **1991**, *113*, 4039−4040.


10.1021/ja035916v CCC: $25.00 

***Scheme 1***

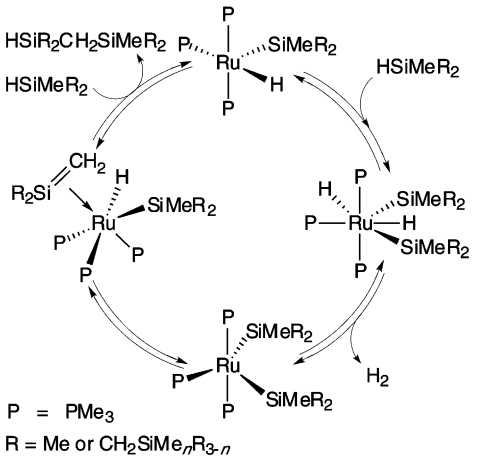


$\beta$-hydrogen elimination from a silyl ligand in $(PMe_3)_3Ru(H)(SiMe_3)$ (**1**) to form silene complex $(PMe_3)_3Ru(CH_2{=}SiMe_2)(H)_2$ (**2**), a process that closely models the key C−H activation step in the catalytic system,[5,6] and provides further evidence in support of the proposed catalytic cycle (Scheme 1). However, $\beta$-hydrogen elimination in **1** cannot lead to formation of a new Si−C bond; rather, productive C−H activation must occur from a 16e$^-$ bis(silyl), $(PMe_3)_3Ru(SiMe_3)_2$. This species could in turn be generated by $H_2$ loss from a bis(silyl) dihydride, $(PMe_3)_3Ru(SiMe_3)_2(H)_2$. In principle, interchange of hydride and silyl ligands at a metal center requires only a series of reductive elimination and oxidative addition steps (e.g., $H_2$ elimination and H−$SiR_3$ addition.) Thus, formation of a bis(silyl) dihydride such as $(PMe_3)_3Ru(SiMe_3)_2(H)_2$ from $(PMe_3)_3Ru(SiMe_3)H_3$ or $(PMe_3)_4Ru(SiMe_3)H$ should be straightforward. However, neither $(PMe_3)_3Ru(SiMe_3)_2(H)_2$ nor any other bis(silyl) had been observed previously in the $(PMe_3)_3Ru$ system. Bis(silyl) dihydrides are certainly known for other metals and coordination environments and are generally quite stable. There is a plethora of stable piano−stool complexes, $LM(SiR_3)_2(H)_2$ (e.g., L = $\eta^5$-pentamethylcyclopentadienyl, $\eta^6$-arene, M = Fe, Co, Ru, Rh, Ir, Cr), some of which exhibit classical hydride and silyl ligands[7−19] and others that can be considered nonclassical.[20,21] Stable bis(silyl) dihydride complexes are also common with phosphine and phosphine oxide co-ligands, and again, both nonclassical[22−28] and classical [29−32] bonding has been observed.

The elusive bis(silyl) dihydride complexes in the $(PMe_3)_3Ru$ system are of interest for several reasons. The relative efficiency of productive $H_2$ loss versus H−$SiR_3$ elimination from such a complex would likely have a direct impact on the rate of catalytic dehydrogenative coupling. In addition, stabilization of the ground-state structures by nonclassical H···H or Si···H interactions is of fundamental interest,[33,34] and may also influence the course of the reductive elimination processes.

We now report the synthesis and structures of a series of stable bis(silyl) dihydride ruthenium complexes, $(PMe_3)_3Ru(SiR_3)_2(H)_2$ ($(SiR_3)_2$ = $(SiH_2Ph)_2$, **3a**; $(SiHPh_2)_2$, **3b**; $(SiMe_2CH_2CH_2SiMe_2)$, **3c**) and in situ spectroscopic characterization of the catalytic intermediate $(PMe_3)_3Ru(SiMe_3)_2(H)_2$, **3d**, at low temperatures. Reductive elimination processes in the bis(silyl) complexes have also been probed through substitution reactions with CO and $PMe_3$.

## Results

**Synthesis and Solution Structures of Stable Ruthenium Bis(silyl) Dihydride Complexes.** Complexes containing monodentate silyls, **3a** and **3b**, were synthesized from $(PMe_3)_3Ru(SiMe_3)H_3$ (**4a**) and the corresponding silane (eq 1). Excess of silane is required to avoid contamination with monosilyl complexes, e.g., $(PMe_3)_3Ru(SiHPh_2)H_3$, an intermediate in the formation of **3b**.

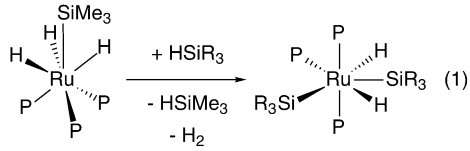


**4a** **3a**, $SiR_3 = SiH_2Ph$

P = $PMe_3$ **3b**, $SiR_3 = SiHPh_2$

The $^1$H spectrum of **3a** at 225 K exhibits chemically inequivalent Ru−H ($\delta$ −9.20, dt; $\delta$ −6.95, dm) and Si−H

(2) Procopio, L. J.; Mayer, B.; Plössl, K.; Berry, D. H. *Polym. Prepr. Am. Chem. Soc., Div. Polym. Chem.* **1992**, *33*, 1241−1242.
(3) Djurovich, P. I.; Dolich, A. R.; Berry, D. H. *J. Chem. Soc., Chem. Commun.* **1994**, 1897−1898.
(4) Ezbiansky, K.; Djurovich, P. I.; LaForest, M.; Sinning, D. J.; Zayes, R.; Berry, D. H. *Organometallics* **1998**, *17*, 1455−1457.
(5) Dioumaev, V. K.; Plössl, K.; Carroll, P. J.; Berry, D. H. *J. Am. Chem. Soc.* **1999**, *121*, 8391−8392.
(6) Dioumaev, V. K.; Ploessl, K.; Carroll, P. J.; Berry, D. H. *Organometallics* **2000**, *19*, 3374−3378.
(7) Fernandez, M. J.; Maitlis, P. M. *Organometallics* **1983**, *2*, 164−165.
(8) Ruiz, J.; Bentz, P. O.; Mann, B. E.; Spencer, C. M.; Taylor, B. F.; Maitlis, P. M. *J. Chem. Soc., Dalton Trans.* **1987**, 2709−2713.
(9) Ricci, J. S., Jr.; Koetzle, T. F.; Fernandez, M. J.; Maitlis, P. M.; Green, J. C. *J. Organomet. Chem.* **1986**, *299*, 383−389.
(10) Bentz, P. O.; Ruiz, J.; Mann, B. E.; Spencer, C. M.; Maitlis, P. M. *J. Chem. Soc., Chem. Commun.* **1985**, 1374−1375.
(11) Fernandez, M. J.; Bailey, P. M.; Bentz, P. O.; Ricci, J. S.; Koetzle, T. F.; Maitlis, P. M. *J. Am. Chem. Soc.* **1984**, *106*, 5458−5463.
(12) Fernandez, M. J.; Maitlis, P. M. *J. Chem. Soc., Dalton Trans.* **1984**, 2063−2066.
(13) Fernandez, M. J.; Maitlis, P. M. *J. Chem. Soc., Chem. Commun.* **1982**, 310−311.
(14) Yao, Z.; Klabunde, K. J.; Asirvatham, A. S. *Inorg. Chem.* **1995**, *34*, 4, 5289−5294.
(15) Asirvatham, V. S.; Yao, Z.; Klabunde, K. J. *J. Am. Chem. Soc.* **1994**, *116*, 5493−5494.
(16) Djurovich, P. I.; Carroll, P. J.; Berry, D. H. *Organometallics* **1994**, *13*, 2551−2553.
(17) Duckett, S. B.; Haddleton, D. M.; Jackson, S. A.; Perutz, R. N.; Poliakoff, M.; Upmacis, R. K. *Organometallics* **1988**, *7*, 1526−1532.
(18) Duckett, S. B.; Perutz, R. N. *J. Chem. Soc., Chem. Commun.* **1991**, 28−31.
(19) Brookhart, M.; Grant, B. E.; Lenges, C. P.; Prosenc, M. H.; White, P. S. *Angew. Chem., Int. Ed. Engl.* **2000**, *39*, 1676−1679.
(20) Jagirdar, B. R.; Palmer, R.; Klabunde, K. J.; Radonovich, L. J. *Inorg. Chem.* **1995**, *34*, 278−283.
(21) Corey, J. Y.; Braddock-Wilking, J. *Chem. Rev.* **1999**, *99*, 175−292.
(22) Luo, X.-L.; Crabtree, R. H. *J. Am. Chem. Soc.* **1989**, *111*, 2527−2535.
(23) Sabo-Etienne, S.; Hernandez, M.; Chung, G.; Chaudret, B.; Castel, A. *New J. Chem.* **1994**, *18*, 175−177.
(24) Delpech, F.; Sabo-Etienne, S.; Chaudret, B.; Daran, J.-C. *J. Am. Chem. Soc.* **1997**, *119*, 3167−3168.
(25) Delpech, F.; Sabo-Etienne, S.; Donnadieu, B.; Chaudret, B. *Organometallics* **1998**, *17*, 4926−4928.
(26) Hussein, K.; Marsden, C. J.; Barthelat, J.-C.; Rodriguez, V.; Conejero, S.; Sabo-Etienne, S.; Donnadieu, B.; Chaudret, B. *Chem. Commun.* **1999**, 1315−1316.
(27) Delpech, F.; Sabo-Etienne, S.; Daran, J.-C.; Chaudret, B.; Hussein, K.; Marsden, C. J.; Barthelat, J.-C. *J. Am. Chem. Soc.* **1999**, *121*, 6668−6682.
(28) Loza, M. L.; de Gala, S. R.; Crabtree, R. H. *Inorg. Chem.* **1994**, *33*, 5073−5078.
(29) Tanke, R. S.; Crabtree, R. H. *Organometallics* **1991**, *10*, 415−418.
(30) Howard, J. A. K.; Keller, P. A.; Vogt, T.; Taylor, A. L.; Dix, N. D.; Spencer, J. L. *Acta Crystallogr., Sect. B: Struct. Sci.* **1992**, *B48*, 438−444.
(31) Nagashima, H.; Tatebe, K.; Ishibashi, T.; Nakaoka, A.; Sakakibara, J.; Itoh, K. *Organometallics* **1995**, *14*, 2868−2879.
(32) Loza, M.; Faller, J. W.; Crabtree, R. H. *Inorg. Chem.* **1995**, *34*, 2937−2941.
(33) Schubert, U. *Adv. Organomet. Chem.* **1990**, *30*, 151−187.
(34) Lin, Z. *Chem. Soc. Rev.* **2002**, *31*, 239−245.

***Table 1.*** Activation Parameters for Intramolecular Exchange of Inequivalent Hydride- and Silyl-Ligands in **3a**, **3b**, and **3d** by NMR Line Shape Analysis

| compd | temperature range, K | $\Delta H^{\ddagger}$, kcal·mol$^{-1}$ | $\Delta S^{\ddagger}$, cal·mol$^{-1}$·K$^{-1}$ |
|---|---|---|---|
| **3a**[a] | 245.8 to 318.7 | $9.3 \pm 0.3$ | $-26 \pm 1$ |
| **3b**[b] | 282.2 to 324.7 | $9.9 \pm 0.6$ | $-13 \pm 2$ |
| **3d**[c] | 148.0 to 179.6 | $6.5 \pm 0.6$ | $-4 \pm 2$ |

[a] RuH and SiH signals were used in the line shape analysis. [b] Only SiH signals were used in the line shape analysis. [c] Only RuH signals were used in the line shape analysis.

resonances ($\delta$ 4.81, br q; $\delta$ 5.57, septet). Two distinct phosphine environments in a 1:2 ratio ($\delta$ −15.2, t; $\delta$ −5.9, d) are observed even at room temperature. These data are consistent with the pentagonal bipyramidal seven-coordinate geometry containing axial phosphines suggested by the solid-state structure (vide infra). The IR stretching frequencies of the RuH and SiH ligands fall in the range of classical terminal hydrides ((Nujol) $\nu$(SiH) = 2031, 2006 cm$^{-1}$, $\nu$(RuH) = 1952 and 1861 cm$^{-1}$) and do not suggest strong agostic Si···H or H···H interactions.[21,33] Compound **3a** is fluxional at higher temperatures, and the pairs of inequivalent RuH and $SiH_2Ph$ groups undergo intramolecular exchange. Coalescence of the ruthenium hydrides is observed at ca. 294 K, whereas the Si−H resonances coalesce at ca. 276 K. Activation parameters were obtained via line shape analysis of the VT $^1$H NMR data between 245.8 and 318.7 K (Table 1). Coalescence of the phosphine ligands was not observed (<325 K). The $^{29}$Si spectrum of **3a** at 25 °C shows a single broad resonance at $\delta$ −15.8. Compound **3a** does not undergo intermolecular exchange with free $PhSiH_3$ on the NMR time scale in the temperature range examined (<325 K).

The bis(diphenylsilyl) complex **3b** exhibits spectral properties very similar to those of **3a**, and likely adopts a comparable geometry. This derivative is also fluxional on the NMR time scale, and coalescence is observed at ca. 305 and 294 K for RuH and SiH signals respectively (Table 1). A product of the first stage in the synthesis of **3b**, the monosilyl complex $(PMe_3)_3Ru(SiHPh_2)H_3$, was readily identified by $^1$H NMR spectroscopy. In particular, the AA′A″XX′X″ pattern for the $PMe_3$ and RuH groups, and a single $SiHPh_2$ ligand are characteristic.[35−44]

The bis(silyl) dihydride complex containing chelating silyl groups, $(PMe_3)_3Ru(SiMe_2CH_2CH_2SiMe_2)(H)_2$ (**3c**), was prepared in 85% yield from the reaction of $(PMe_3)_4Ru(SiMe_3)H$ and $HSiMe_2CH_2CH_2SiMe_2H$ at room temperature (eq 2). An intermediate complex, possibly the initial product of silyl/silane exchange, $(PMe_3)_4Ru(H)(SiMe_2CH_2CH_2SiMe_2H)$, was observed at 220 K by $^1$H NMR after 1 min reaction at room temperature. This intermediate readily converts into **3c**, via loss of phosphine and chelation of the second silicon hydride at room temperature (eq 2).

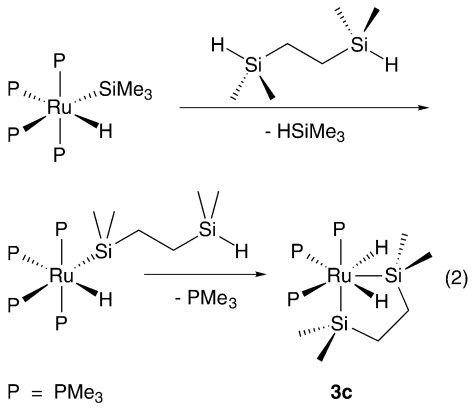


The complex of the chelating bis(silyl), **3c**, exhibits rather different spectral features than **3a** and **3b**. A singlet resonance is observed for the two hydrides down to 150 K in the $^1$H NMR, and the pairs of $SiMe_2$ and $CH_2$ groups also exhibit single environments in the $^1$H, $^{13}$C, and $^{29}$Si spectra. Furthermore, the three phosphine ligands also appear as a single resonance in the $^{31}$P NMR spectrum ($\delta$ −11.49 at 180 K). However, two distinct hydride stretches are observed in IR spectrum (Nujol) at 1940 and 1740 cm$^{-1}$. The former is due to a classical RuH ligand, and the lower energy band is consistent with a nonclassical Ru···H···Si interaction.[21,33] Again, no intermolecular exchange with free silane was detected on the NMR time scale up to 353 K (200 MHz, $^1$H NMR). The unsymmetrical ground-state structure suggested by the IR spectrum — but not evident by NMR — is supported by the solid-state structure (vide infra), indicating **3c** is highly fluxional in solution, even at 150 K.

**Observation and Solution Structure of the Unstable Bis(silyl) Dihydride Complex, $(PMe_3)_3Ru(SiMe_3)_2(H)_2$ (3d).** Attempts to prepare or observe the bis(trimethylsilyl) complex analogous to **3a**−**c** by reaction of $HSiMe_3$ with either $(PMe_3)_3Ru(SiMe_3)H_3$ or $(PMe_3)_4Ru(SiMe_3)H$ were unsuccessful. No reaction is observed at temperatures below ca. 60 °C, and catalytic dehydrocoupling to carbosilanes occurs at higher temperatures. Only $(PMe_3)_3Ru(SiMe_3)H_3$ is observed as the resting state of the catalyst. Given the facile reactions of these ruthenium complexes with less hindered or chelating silanes described above, it seems likely that steric congestion destabilizes $(PMe_3)_3Ru(SiMe_3)_2(H)_2$ (**3d**) relative to $(PMe_3)_3Ru(SiMe_3)H(L)$ (L = $PMe_3$, $(H)_2$), resulting in unfavorable equilibria.

We have recently reported isolation of the highly reactive 16e$^-$ complex, $(PMe_3)_3Ru(SiMe_3)H$, **1**, which is in equilibrium with the 18e$^-$ silene complex $(PMe_3)_3Ru(CH_2SiMe_2)(H)_2$, **2**, and also forms weak adducts with dinitrogen, **1-N$_2$** (eq 3).[5,6]

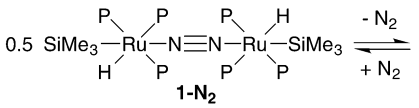


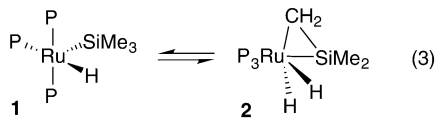


(35) Gilbert, S.; Knorr, M.; Mock, S.; Schubert, U. *J. Organomet. Chem.* **1994**, *480*, 241−254.
(36) Hubler, K.; Hubler, U.; Roper, W. R.; Schwerdtfeger, P.; Wright, L. J. *Chem. Eur. J.* **1997**, *3*, 1608−1616.
(37) Knorr, M.; Gilbert, S.; Schubert, U. *J. Organomet. Chem.* **1988**, *347*, C17−C20.
(38) Mohlen, M.; Rickard, C. E. F.; Roper, W. R.; Salter, D. M.; Wright, L. J. *J. Organomet. Chem.* **2000**, *593*−*594*, 458−464.
(39) Rickard, C. E. F.; Roper, W. R.; Woodgate, S. D.; Wright, L. J. *J. Organomet. Chem.* **2000**, *609*, 177−183.
(40) Schubert, U.; Gilbert, S.; Mock, S. *Chem. Ber.* **1992**, *125*, 835−837.
(41) Burn, M. J.; Bergman, R. G. *J. Organomet. Chem.* **1994**, *472*, 43−54.
(42) Procopio, L. J., Ph.D. Thesis, University of Pennsylvania, 1991.
(43) Dioumaev, V. K.; Procopio, L. J.; Carroll, P. J.; Berry, D. H. *J. Am. Chem. Soc.* **2003**, accepted for publication.
(44) Yardy, N. M.; Lemke, F. R.; Brammer, L. *Organometallics* **2001**, *20*, 5670−5674.

In theory, reaction of **1** with $HSiMe_3$ should yield **3d**, without competing equilibria involving $PMe_3$ or $H_2$ association. However, treatment of **1** with $HSiMe_3$ at room temperature leads to stoichiometric formation of $(PMe_3)_3Ru(SiMe_2CH_2SiMe_3)H_3$, **4b**, and subsequent exchange of the silyl ligand with excess $HSiMe_3$ to yield $HSiMe_2CH_2SiMe_3$ and **4a** (eq 4). Compound **4b** is an empirical isomer of **3d** resulting from dehydrocoupling of two equiv $HSiMe_3$. The interconversion of **4a** and **4b** by exchange of silyl ligands was independently demonstrated by reacting either complex with the corresponding free silane. An equilibrium constant of ca. 9 favoring **4a** was obtained starting from either complex at ambient temperatures, reflecting the greater steric hindrance of the carbosilyl ligand in **4b**. For preparative purposes, **4b** was independently synthesized in essentially quantitative yield from **4a** by ligand exchange with $HSiMe_2CH_2SiMe_3$ and periodical removal of $HSiMe_3$ (eq 4). The NMR features of **4b** closely resemble that of the previously described **4a**[42,43] and other $L_3M(ER_3)H_3$ complexes.[35−41] The spectroscopic assignment was confirmed by single-crystal X-ray diffraction analysis, vide infra.

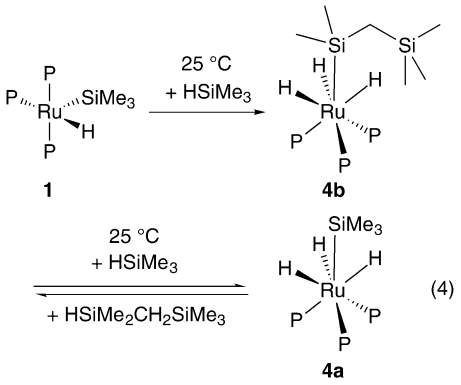


**1** **4b** **4a**

Given the apparent instability of **3d**, it was necessary to examine the reaction of the 16e⁻ complex **1** with $HSiMe_3$ at low temperatures. Note that generation of unligated **1** at low temperatures is complicated by slow rates of dinitrogen dissociation from **1-N₂** and interconversion of **1** with **2**. However, by dissolving solid **1-N₂** in methylcyclohexane-$d_{14}$, rapidly degassing at −10 °C, adding $HSiMe_3$, and introduction of the tube into the cold probe of the NMR spectrometer it was possible to generate solutions containing ca. 12% **1-N₂**, 55% of **2**, and 33% of the initial reaction product, $(PMe_3)_3Ru(SiMe_3)_2(H)_2$, **3d**. The residual dinitrogen and silene complexes are essentially unreactive up to 190 and 260 K, respectively. The $^1H$ NMR spectrum of **3d** at 155 K exhibits two multiplets for inequivalent ruthenium hydrides at $\delta$ −9.56 and −7.48, although coupling to the phosphines is poorly resolved due to the solvent viscosity at 155 K. Inequivalent $SiMe_3$ groups are observed at $\delta$ 0.18 and 0.32. Significantly, resonances for excess $HSiMe_3$ are unperturbed at this low temperature, and the Si−H is observed as a fairly sharp resonance at $\delta$ 3.98 ($\nu_{1/2}$ = 17 Hz). The $^{31}P$ spectrum of **3d** (155 K) exhibits two resonances in a 2:1 ratio. These spectral features are extremely similar to those for **3a**,**b** and are consistent with an analogous pentagonal bipyramidal structure with both silyl groups located in the equatorial plane.

As observed for **3a** and **3b**, **3d** exhibits dynamic NMR behavior at higher temperatures; however, in this instance several additional intermolecular processes begin to occur within

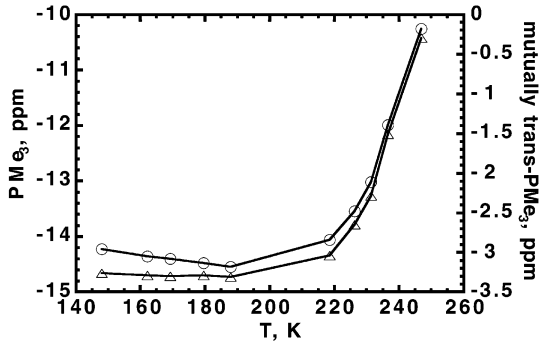


***Figure 1.*** Temperature dependence of the averaged $^{31}P$ NMR chemical shifts of **3d** and **1**. The $\delta$ values for the axial mutually trans phosphines are plotted as triangles and the equatorial phosphines as circles.

***Table 2.*** $^{31}P$ NMR Chemical Shifts and Calculated Concentrations for the Equilibrium Mixture of **1** and **3d**

| | observed $^{31}P$ NMR resonances | | calculated [**3d**], | calculated [**1**], |
|---|---|---|---|---|
| *T*, K | ppm | | mM | mM |
| 148 | −3.26 | −14.23 | 10.40 | <0.01 |
| 162 | −3.29 | −14.36 | 10.40 | <0.01 |
| 169 | −3.30 | −14.40 | 10.40 | <0.01 |
| 180 | −3.29 | −14.48 | 10.39 | <0.01 |
| 188 | −3.31 | −14.55 | 10.38 | 0.02 |
| 219 | −3.04 | −14.06 | 13.54 | 0.86 |
| 226 | −2.65 | −13.54 | 12.78 | 1.62 |
| 231 | −2.29 | −13.02 | 12.03 | 2.37 |
| 237 | −1.51 | −11.99 | 10.34 | 3.12 |
| 247 | −0.30 | −10.26 | 5.61 | 3.73 |

distinct temperature regimes. As the temperature is raised to 162 K, the Ru−H resonances show dynamic broadening, but the Si−H resonance of free silane remains unperturbed. Coalescence of the ruthenium hydrides to a single peak at $\delta$ −8.50 is observed at 180 K, whereas the free silane shows only slight broadening ($\delta$ 3.98, $\nu_{1/2}$ = 39 Hz) at this temperature. However, a slight increase in temperature to 188 K leads to a dramatic broadening of the free silane resonance ($\delta$ 3.92, $\nu_{1/2}$ = 388 Hz). At 219 K, the individual resonances for the ruthenium and silicon hydrides have disappeared, replaced with a broad peak at ca. $\delta$ 1.7 ($\nu_{1/2}$ = 400 Hz). This chemical shift is consistent with the weighted average of the two Ru−H's and the excess silane hydride, and the chemical shift does change with $HSiMe_3$ concentration in separate experiments. Line shape analysis of the hydride resonances indicate that two independent processes are occurring: intramolecular exchange of the two Ru−H's (Table 1), and with a higher barrier, intermolecular exchange with free $HSiMe_3$. The latter process is most likely due to reversible Si−H reductive elimination to regenerate the 16e⁻ starting complex, **1** (eq 5). Complementary information for the dissociation of $HSiMe_3$ from **3d** can be obtained from $^{31}P$ NMR.

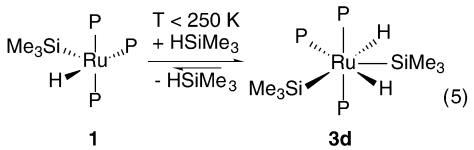


**1** **3d**

The temperature dependence of the averaged $^{31}P$ NMR chemical shifts of **3d** and **1** in the presence of ca. 9 equiv excess $HSiMe_3$ is shown in Figure 1 and summarized in Table 2. The chemical shifts of the two phosphine resonances remain fairly

constant between 148 and 188 K and constitute the limiting low-temperature spectrum of **3d**. As the temperature is raised from 188 to 247 K the resonances undergo a substantial drift (4 ppm) to lower field. This behavior is consistent with the proposed dynamic exchange between **1** and **3d**, with **1** being present in increasingly significant quantities at higher temperatures. Knowing the limiting low-temperature chemical shifts for both **1**[45] and **3d**, the equilibrium constant for $HSiMe_3$ dissociation from **3d** can be calculated at each temperature, and thermodynamic parameters extracted from the temperature dependence of $K_d$. The values determined, $\Delta H_{SiH-elim} = 11.0 \pm 0.6$ kcal·mol$^{-1}$ and $\Delta S_{SiH-elim} = 40 \pm 2$ cal·mol$^{-1}$·K$^{-1}$, are consistent with the proposed dissociative process. Furthermore, the equilibrium concentrations of **1** and **3d** determined from the $^{31}P$ NMR can be utilized in the $^1H$ NMR line shape analysis to determine the activation parameters for $HSiMe_3$ dissociation ($\Delta H^{\ddagger}_{SiH-elim} = 9.2 \pm 0.8$ kcal·mol$^{-1}$; $\Delta S^{\ddagger}_{SiH-elim} = 9 \pm 3$ cal·mol$^{-1}$·K$^{-1}$; $\Delta H^{\ddagger}_{SiH-add} = -1.8 \pm 0.8$ kcal·mol$^{-1}$; $\Delta S^{\ddagger}_{SiH-add} = -31 \pm 3$ cal·mol$^{-1}$·K$^{-1}$).

From the previous analysis, it is clear that substantial concentrations of **1** are present in solutions of **3d** at higher temperatures, even in the presence of excess $HSiMe_3$. Furthermore, this highly reactive unsaturated species can do more than merely re-coordinate $HSiMe_3$. Proton NMR spectra of **3d** held at 262 K for hours reveal the appearance of several new resonances between $\delta$ −2 and −15 ppm, suggesting the formation of a variety of new ruthenium hydride species. Two of the species produced are known complexes and can be conclusively identified: **4a** and $(PMe_3)_4Ru(SiMe_3)H$. These 18e$^-$ complexes are the net result of reaction of **1** with $H_2$ and $PMe_3$, respectively. As there is no apparent source of these ligands other than **3d** (and **1**) under these reaction conditions, the stoichiometry suggests that additional complexes containing $[(PMe_3)_2Ru]$ and $[(PMe_3)_3Ru(SiMe_3)_2]$ fragments are concurrently produced. Note that the concentration of silene complex **2** (present from the original sample preparation, vide supra) does not change significantly at this temperature, and that formation of $HSiMe_2CH_2SiMe_3$ (and $H_2$) by dehydrocoupling is slow and cannot account for the increase in $(PMe_3)_3Ru(SiMe_3)H_3$. The redistribution of ligands is not readily reversible: cooling the sample from 262 K back to 155 K allows clearer analysis of all species in the $^1H$ NMR spectrum, but only a small fraction of **3d** is observed.

The phosphine and silyl methyl regions of the $^1H$ NMR spectrum of this complex mixture cannot be evaluated with total confidence, thus identification of the various species present must be viewed as tentative. However, the number of hydride resonances and associated phosphine coupling patterns (confirmed in the $^1H\{^{31}P\}$ spectra) provide further information and permit *tentative* assignment consistent with the apparent stoichiometry of the ligand redistribution processes. Furthermore, repeated generation of redistribution mixtures in independent experiments and with different initial concentrations of $HSiMe_3$ allows correlation of the hydride resonances with peaks in the silicon methyl region of the $^1H$ NMR spectra, as well as peaks in the $^{31}P$ spectra.

When the solution containing **3d**, generated from **1** and $HSiMe_3$ at 195 K as described above, is held at 262 K for 1.5 h, three major species appear in a ratio of approximately 10:8:1. One of them can be tentatively assigned as the $(PMe_3)_2Ru(SiMe_3)_3H_3$ (**I**). Complex **I** exhibits a nonfirst-order multiplet at $\delta$ −9.13, and a single $SiMe_3$ resonance at $\delta$ 0.01 in $^1H$ NMR; these two peaks are found in a 1:9 ratio, suggesting a stoichiometry of one Ru−H for each $SiMe_3$. The simplest new 18e$^-$ complex with a 1:1 Ru−H/$SiMe_3$ ratio is $(PMe_3)_2Ru(SiMe_3)_3H_3$ — derived from **3d** through a phosphine loss and $HSiMe_3$ addition. Another possibility is the 16e$^-$ intermediate, $(PMe_3)_2Ru(SiMe_3)_2(H)_2$.

The other major product of ligand redistribution (**II**) exhibits two ruthenium hydride resonances, coupled inequivalently to two phosphorus nuclei ($\delta$ −10.01, dd, $J_{PH} = 21$, 34 Hz; $\delta$ −12.17, dd, $J_{PH} = 24$, 64 Hz). The two d of d coupling patterns collapse to singlets in the $^1H\{^{31}P\}$ spectrum. Two $^1H$ resonances for $SiMe_3$ groups are observed at $\delta$ 0.12 and 0.09, each integrating as 18:1 against each of the hydride resonances. This may be interpreted as a complex with an overall $SiMe_3$/Ru−H ratio of 4:2 (e.g., $(PMe_3)_2Ru(SiMe_3)_4(H)_2$, possessing two different $SiMe_3$ and hydride environments). The considerable steric crowding in **II** finds some precedent in $(PMe_3)_4Ru(GeMe_3)_2$,[46] in which six large ligands surround the ruthenium center. Furthermore, although complex **II** would formally be an eight-coordinate Ru(VI) species, the presence of one or two fluxional $\eta^2$-$HSiMe_3$ ligands would serve to reduce both crowding and the formal oxidation state. Further speculation is unwarranted, due to the possibility of unobserved peaks (obscured or in coalescence) and other uncertainties.

The concentration of the third redistribution product (**III**) is low, but can be increased significantly (**I**:**II**:**III** ratio ca. 3:2:2) by removal of volatiles (including $HSiMe_3$) from the cold sample of **3d** and addition of fresh cold solvent. Complex **III** exhibits a singlet $^1H$ resonance at $\delta$ −1.56, a nonfirst-order multiplet at $\delta$ −9.31, and two singlet $SiMe_3$ resonances at $\delta$ 0.19, 0.42 in a 2:2:9:9 ratio. The $\delta$ −1.56 resonance falls in a region far downfield from classical ruthenium hydrides or even nonclassical $\eta^2$-Si−H complexes.[21] For example, $(PCy_3)_2Ru(\eta^2\text{-}H{-}SiR_3)_2(H)_2$ complexes reported by Sabo-Etienne and coworkers exhibit chemical shifts for the nonclassical Ru−H−Si hydrides only a few ppm downfield from the classical ruthenium hydrides (ca. $\delta$ −7 to −10 vs ca. $\delta$ −10 to −13).[24,27] However, another class of ligands, $\eta^2$-($H_2$), show a wide range of chemical shifts[47,48] encompassing the $\delta$ −1.56 observed in **III** (e.g., $\delta$ −1.70 in $(P^iPr_3)_2(CO)Ru(SiEt_3)Cl(\eta^2\text{-}H_2)$[49] and $\delta$ −2.4 $[(dppm)_2HRu(\eta^2\text{-}H_2)]^+[OPh]^-$[50]). We can then formulate a tentative assignment of **III** as $(PMe_3)_2Ru(SiMe_3)_2(H)_2(\eta^2\text{-}H_2)$ or $(PMe_3)_2Ru(\eta^2\text{-}H{-}SiMe_3)_2(\eta^2\text{-}H_2)$. Either formulation can accommodate the constraint that the two $SiMe_3$ environments must be inequivalent.

Remarkably, despite the plethora of ruthenium silyl hydride complexes present at 262 K, the situation reverts to extreme simplicity after samples are warmed to room temperature; **4a** and **4b** are the only ruthenium products observed. The silene

(45) In the absence of $HSiMe_3$, **1** exhibits two phosphine resonances ($^{31}P$ NMR, 303 K, $\delta$ 5.58, d and −3.31 t), which show only a slight temperature dependence ($\delta$ 5.58, d and −2.56, t at 166 K) and do not undergo dynamic broadening or lose the P−P coupling.

(46) Reichl, J. A.; Popoff, C. M.; Gallagher, L. A.; Remsen, E. E.; Berry, D. H. *J. Am. Chem. Soc.* **1996**, *118*, 9430−9431.
(47) Heinekey, D. M.; Oldham, W. J., Jr. *Chem. Rev.* **1993**, *93*, 913−926.
(48) Sabo-Etienne, S.; Chaudret, B. *Chem. Rev.* **1998**, *98*, 2077−2091.
(49) Esteruelas, M. A.; Oro, L. A.; Valero, C. *Organometallics* **1991**, *10*, 462−466.

complex present at 262 K from the initial generation of **3d** reacts (via **1**) with $HSiMe_3$ at a significant rate above 273 K, and is consumed rapidly at ambient temperatures. Approximately stoichiometric amounts of the carbosilane dehydrocoupling product are observed as **4b** and free $HSiMe_2CH_2SiMe_3$. Note that no other species are observed when the sample is re-cooled to 262 K after a day at room temperature.

**Reactivity.** It was shown above that **3d** undergoes rapid and reversible elimination of $HSiMe_3$ at temperatures above 220 K, and that substantial amounts of the 16e$^-$ **1** is present at higher temperatures. It is not surprising, therefore, that solutions of **3d** react rapidly with carbon monoxide. The kinetic product is *mer*-$(PMe_3)_3Ru(H)(SiMe_3)(CO)$, a monocarbonyl complex in which the CO ligand is located trans to the $SiMe_3$ group, analogous to the geometry at ruthenium in **1-N$_2$**. At room temperature, however, isomerization to the more stable *fac*-$(PMe_3)_3Ru(H)(SiMe_3)(CO)$ is complete in <1 h (eq 6).[5,42]

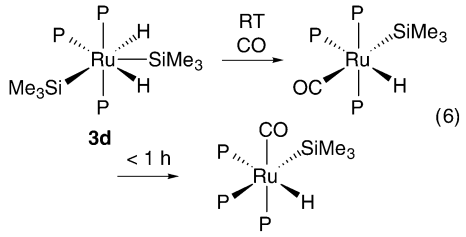


Although bis(silyl) dihydride complexes **3a**−**c** are quite stable relative to **3d**, they are also labile and readily react with CO following elimination of $HSiR_3$ and/or $H_2$. For example, reaction of bis(diphenylsilyl) derivative **3b** under 1 atm CO is complete within 10 min at room temperature, yielding $(PMe_3)_3Ru(H)(SiHPh_2)(CO)$ as a mixture of three isomers: mer (trans CO, Si), fac, and mer (trans CO, H) (eq 7). The ratio after 10 min is 80:14:6 and changes to 40:50:10 after 1 h, again reflecting the greater stability of the fac-isomer. As expected, reaction of **3b** with $PMe_3$ follows the same trend to give a single product of SiH elimination − $(PMe_3)_4Ru(SiHPh_2)H$. The chelating bis(silyl) **3c** behaves similarly, although significantly more slowly. Approximately 10% conversion to the mer-isomer $(PMe_3)_3(CO)Ru(SiMe_2CH_2CH_2SiMe_2H)H$ is achieved after 10 min (1 atm CO, 25 °C). After 24 h (100% conversion) the fac-isomer is predominant (fac/mer = ca. 25).

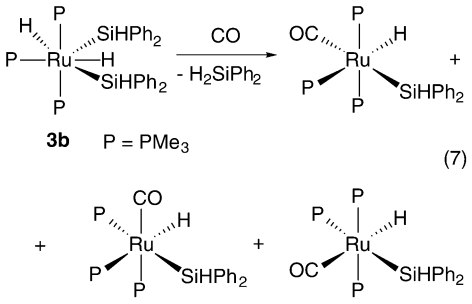


The formation of mer-monocarbonyl complexes (primarily CO trans to $SiR_3$) as the kinetic products in the above reactions suggests that the five-coordinate intermediates, $(PMe_3)_3Ru(H)(SiR_3)$, maintain a square pyramidal geometry with the silyl predominantly trans to the vacant coordination site, as suggested by the spectral features of **1** and by the structure of **1-N$_2$**. The greater stability of the fac-isomers presumably reflects the unfavorable arrangement of two strong trans-directing ligands − silyl and CO − in the kinetic mer-isomers.

***Scheme 2***

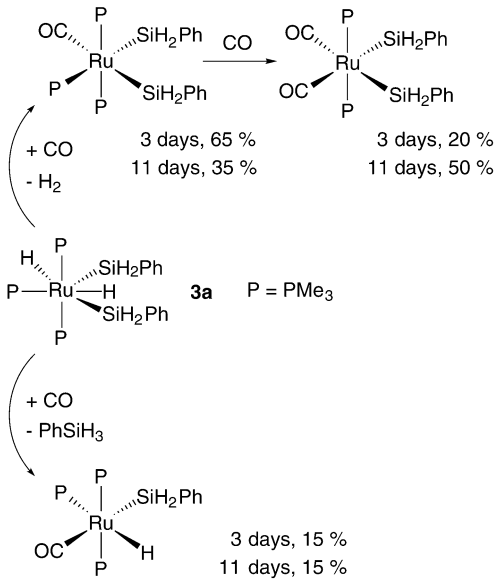


Although bis(silyl) complexes **3b**−**d** react with CO only via silane loss, reaction of **3a** with CO is more complex. Carbonyl derivatives arising from both SiH and $H_2$ elimination are observed (Scheme 2). The former produces a monocarbonyl complex, *mer*-$(PMe_3)_3Ru(H)(SiHPh_2)(CO)$, which does not undergo isomerization to the fac-isomer after weeks at room temperatures. The majority of the reaction, however, proceeds by $H_2$ elimination to generate a monocarbonyl bis(silyl) derivative, *mer*-$(PMe_3)_3(CO)Ru(SiH_2Ph)_2$. Subsequent substitution of a second phosphine ligand trans to silyl produces the dicarbonyl complex, $(PMe_3)_2(CO)_2Ru(SiH_2Ph)_2$ (cis carbonyls and silyls, trans phosphines). The relative ratio of $H_2$ vs HSi elimination can be estimated from the sum of *mer*-$(PMe_3)_3(CO)Ru(SiH_2Ph)_2$ and $(PMe_3)_2(CO)_2Ru(SiH_2Ph)_2$ vs *mer*-$(PMe_3)_3Ru(H)(SiHPh_2)(CO)$ as approximately 85:15. The facile formation of the dicarbonyl complex in this particular case is mostly due to the strong trans effect of the second silyl on the phosphine, a factor not present in the substitution reactions of **3b**−**d**.

**Solid State Structures.** The structure of the bis(silyl) dihydride complex **3a** in the solid state was determined by a single-crystal X-ray diffraction study. Selected bond distances and angles are presented in Table 4. As illustrated by the ORTEP diagram (Figure 2), the non-hydrogen ligands around ruthenium form a distorted trigonal bipyramid, with two phosphines trans in the axial positions (P2−Ru−P3 = 171.4(1)°), and third phosphine and the two silyls forming the equatorial plane (sum of angels = 360.0°). Two of the three angles in the equatorial plane are considerably larger (P1−Ru−Si1 = 133.4(1)° and Si1−Ru−Si2 = 133.0(1)°) than the third (P1−Ru−Si2 = 93.6(1)°). The ruthenium hydrides were not located, but can reasonably be assumed to fill the substantial voids in the equatorial plane located on both sides of Si1, thus completing the seven-coordinate pentagonal bipyramidal geometry. Note that inequivalent hydride environments are required by the IR spectrum and the low-temperature NMR spectra exhibited by **3a**. The Ru−P bond length for the equatorial phosphine (2.386(2) Å) is longer than for the axial ligands (2.339(2), 2.329(2) Å) consistent with the strong trans influence of silicon

***Table 3.*** Crystal Data for **3a**, **3c**, and **4b**

| compound | **3a** | **3c** | **4b** |
|---|---|---|---|
| formula | $RuC_{21}H_{43}Si_2P_3$ | $Ru_1C_{15}H_{45}Si_2P_3$ | $Ru_1C_{15}H_{47}Si_2P_3$ |
| formula weight | 545.73 | 475.67 | 477.69 |
| crystal system | orthorhombic | monoclinic | monoclinic |
| space group | $Pna2_1$ (#33) | $C2/c$ (#15) | $P2_1/n$ (#14) |
| color | pale yellow | colorless | colorless |
| $Z$ | 4 | 8 | 4 |
| $a$, Å | 18.0290(6) | 35.9187(5) | 14.1488(1) |
| $b$, Å | 16.2315(6) | 9.3210(1) | 18.5561(3) |
| $c$, Å | 9.5547(4) | 16.1099(1) | 9.9845(1) |
| $\beta$, deg | | 114.123(1) | 93.059(1) |
| $V$, Å$^3$ | 2796.1(3) | 4922.55(9) | 2617.66(5) |
| $T$, K | ambient | 210 | 200 |
| $R$ | 0.042[a] | 0.0507[b] | 0.0456[b] |
| $wR$ | 0.050[a] | 0.1107[b] | 0.1127[b] |
| GOF | 1.58 | 1.103 | 1.127 |

[a] $F^2 > 3.0\sigma(F^2)$ data used; $R = \sum||F_o| - |F_c||/\sum|F_o|$; $wR = \{\sum w(|F_o| - |F_c|)^2/\sum w|F_o|^2\}^{1/2}$. [b] All data used; $R = \sum(||F_o| - |F_c||)/\sum|F_o|$; $wR = \{\sum w(F_o^2 - F_c^2)^2/\sum w(F_o^2)^2\}^{1/2}$.

***Table 4.*** Selected Bond Distances and Nonbonding Contacts (Å) and Angles (deg) in **3a**

| | | | | | |
|---|---|---|---|---|---|
| Ru−P1 | 2.386(2) | Ru−P2 | 2.339(2) | Ru−P3 | 2.329(2) |
| Ru−Si1 | 2.390(2) | Ru−Si2 | 2.437(2) | | |
| P1−Ru−P2 | 94.2(1) | P1−Ru−Si1 | 133.4(1) | | |
| P1−Ru−P3 | 93.8(1) | P2−Ru−Si1 | 87.3(1) | | |
| P2−Ru−P3 | 171.4(1) | P1−Ru−Si2 | 93.6(1) | | |
| P3−Ru−Si1 | 89.2(1) | P2−Ru−Si2 | 87.9(1) | | |
| P3−Ru−Si2 | 88.7(1) | Si1−Ru−Si2 | 133.0(1) | | |

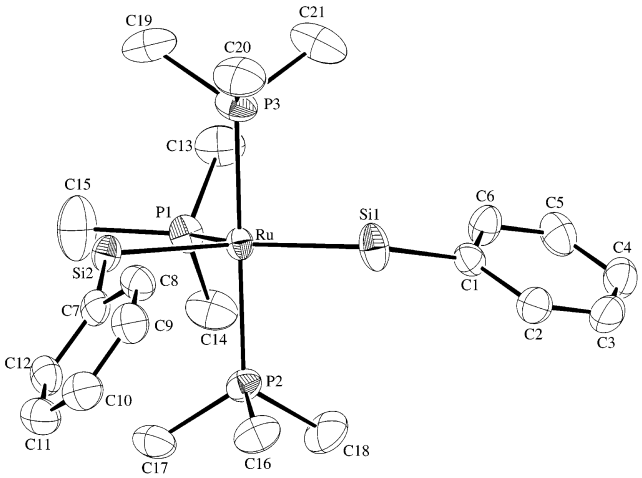


***Figure 2.*** ORTEP drawing of $(PMe_3)_3Ru(SiH_2Ph)_2(H)_2$, **3a**, (30% thermal ellipsoids).

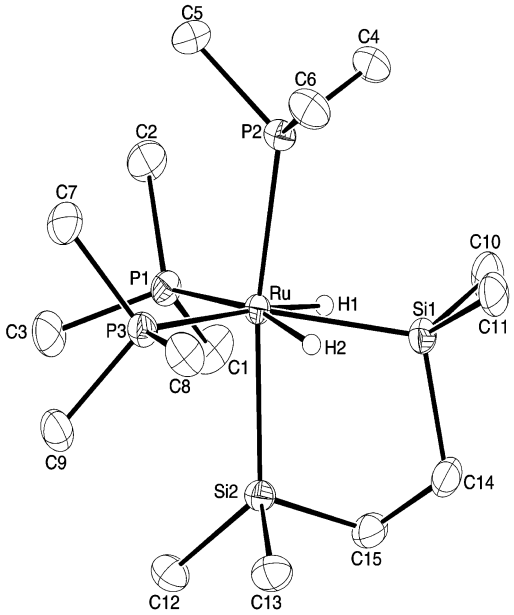


***Figure 3.*** ORTEP drawing of $(PMe_3)_3Ru(SiMe_2CH_2CH_2SiMe_2)(H)_2$, **3c**, (30% thermal ellipsoids).

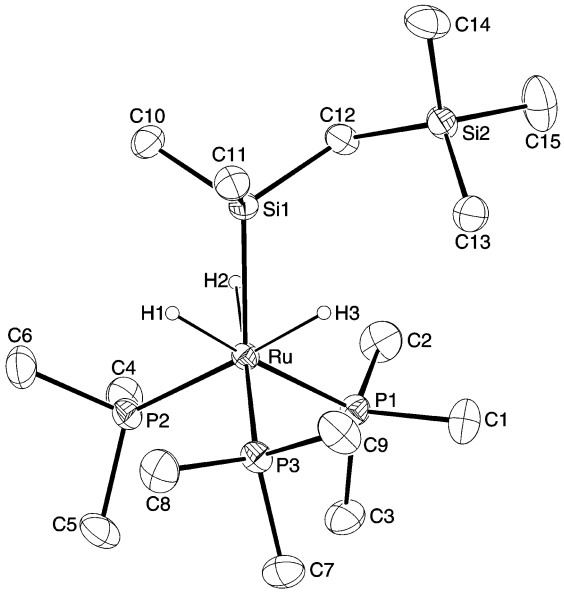


***Figure 4.*** ORTEP drawing of $(PMe_3)_3Ru(SiMe_2CH_2SiMe_3)H_3$, **4b**, (30% thermal ellipsoids).

and hydride ligands.[43] The two Ru−Si bond lengths are also considerably different, with a longer bond observed for the silyl ligand presumed to be approximately trans to a hydride (Ru−Si2 = 2.437(2) Å, Ru−Si1 = 2.390(2) Å).

The crystal structure of the chelating bis(silyl) **3c** also reveals a distorted bipyramidal geometry (Figure 3), but in this case one of the axial positions is occupied by a silyl ligand, and two phosphines and a silyl are located in the equatorial plane (P2−Ru−Si2 = 168.63(3)°, sum of equatorial angles = 358.66°). Selected bond distances and angles are presented in Table 5. The two hydrides were located adjacent to Si1, and were successfully refined isotropically. Although final refinement gave very satisfactory R factors, distances and angles concerning the hydride ligands must still be viewed with appropriate caution, as the positions of hydrogens bound to heavy atoms are often imprecise in X-ray structural determinations. One of the hydrides appears to exhibit an agostic interaction with Si1 (1.81(4) Å), whereas the other is in only moderately close contact with the same silicon (2.15(3) Å). Both silyls are more or less trans to phosphines, hence the Ru−Si distances are similar. The distance for the agostic silyl is only slightly elongated (2.4682 vs 2.4514 Å). Similar structures with two Ru−H···Si contacts to the same Si (one short, 1.73−1.84 Å, and one long, 2.04−2.43 Å) were recently found experimentally and probed computationally by Sabo-Etienne and co-workers.[24,27,51] Furthermore, structures with two $((PCy_3)_2Ru(\eta^2\text{-}H_2)(\eta^2\text{-}H{-}SiPh_3)(H)_2$, 1.72 and 1.83 Å),[26] three $(((PPh_3)_3Ru(H)_2(\eta^2\text{-}H{-}SiPh_2OSi(OH)Ph_2$, 1.97, 2.03 and 2.07 Å),[52] and even four

(50) Ayllon, J. A.; Gervaux, C.; Sabo-Etienne, S.; Chaudret, B. *Organometallics* **1997**, *16*, 2000−2002.
(51) Nikonov, G. I. *Angew. Chem., Int. Ed. Engl.* **2001**, *40*, 3353−3355.

***Table 5.*** Selected Bond Distances and Nonbonding Contacts (Å) and Angles (deg) in **3c**

| | | | | | |
|---|---|---|---|---|---|
| Ru—P1 | 2.3456(9) | Ru—Si1 | 2.4682(9) | Ru—H1 | 1.56(4) |
| Ru—P2 | 2.3689(8) | Ru—Si2 | 2.4514(9) | Ru—H2 | 1.50(4) |
| Ru—P3 | 2.3522(9) | | | Si1—H1 | 1.81(4) |
| P1—Ru—P2 | 98.81(3) | P3—Ru—Si1 | 138.52(3) | | |
| P1—Ru—P3 | 98.84(3) | P1—Ru—Si2 | 92.06(3) | | |
| P3—Ru—P2 | 92.95(3) | P2—Ru—Si2 | 168.63(3) | | |
| P1—Ru—Si1 | 121.30(3) | P3—Ru—Si2 | 88.63(3) | | |
| P2—Ru—Si1 | 90.92(3) | Si2—Ru—Si1 | 80.52(3) | | |
| P1—Ru—H1 | 74.4(14) | P1—Ru—H2 | 168.9(12) | | |
| P2—Ru—H1 | 93.4(13) | P2—Ru—H2 | 92.2(12) | | |
| P3—Ru—H1 | 171.4(13) | P3—Ru—H2 | 78.8(12) | | |
| Si1—Ru—H1 | 47.2(14) | Si1—Ru—H2 | 59.8(12) | | |
| Si2—Ru—H1 | 86.3(13) | Si2—Ru—H2 | 77.1(12) | | |
| H1—Ru—H2 | 107(2) | Ru—Si1—H1 | 39.2(11) | | |

strong interactions ($(P^iPr_3)_2Ru(H)_2(SiH_4)Ru(H)_2(P^iPr_3)_2$, 1.69, 1.69, 1.73, and 1.73 Å)[53] were also reported by the same group. These interactions are believed to be of great importance for the fluxional behavior, reactivity and stability of the complexes. For example, in $(PCy_3)_2Ru(\eta^2\text{-}H_2)(\eta^2\text{-}H{-}SiPh_3)(H)_2$ the two bulky phosphines are forced to adopt an almost cis arrangement (109.71°) to accommodate the two agostic interactions. In all of the aforementioned cases, including **3c**, the short and the long H···Si contacts were detected in solution (IR) as well as in the solid state (X-ray). The calculated model compounds also exhibited a comparable geometry.[24,26,27,53] On the NMR time scale these interactions are masked by fluxional averaging and are manifested only in the increase of the apparent $J_{SiH}$ (22−82 Hz, presumably an average of $^1J_{agostic}$ and $^2J_{classical}$).[24,26,27,53] Noteworthy, the average $J$ value is not a rigorous criterion.[54] Thus, in the case of $((PCy_3)_2Ru(H)_2(\eta^2\text{-}H{-}SiMe_2)_2O)$[24] the agostic interactions have surprisingly little influence on $J_{SiH}$ (22 Hz), where as for **3c** the effect is even less pronounced (16 Hz). However, a $J_{SiH}$ value resulting from the averaging of a classical $^2J_{SiH}$ and an agostic $^1J_{SiH}$ can be especially misleading as these scalar couplings may have opposite signs.

The solid-state structure of the silyl trihydride complex **4b** is shown in Figures 4. Selected bond distances and angles are presented in Table 6. All hydrogens were located and refined isotropically. The crystal structure of this seven-coordinate complex can be formulated as a roughly tetrahedral $P_3Si$ array surrounding ruthenium, with the three hydrides capping the $P_2Si$ faces. This ligand arrangement is typical for such $L_3M(ER_3)H_3$ (E = Si or Sn) complexes.[35−40,42−44,55] The Si−C and Ru−P bonds are eclipsed when the molecule is viewed along the Ru−Si axis, and the hydride ligands are staggered with respect to the Si methyls and P atoms. Alternatively, the structure can be viewed as a pseudooctahedral *fac*-$Ru(PMe_3)_3H_3$ unit with the silyl group capping the face defined by the three hydride ligands. In either case, this arrangement minimizes steric repulsion between the nonhydride ligands around the metal, in much the same manner as the trigonal bipyramidal geometry found for the $RuP_3Si_2$ core in compounds **3a** and **3c**. All distances and angles are within expected range with the exception of shorter than van der Waals contacts between hydrides and Si1 (2.00(4)−2.09(4) Å for H···Si), which may indicate some delocalized bonding in the $Ru(Si)H_3$ fragment, albeit not a strong interaction. The H···H separations (2.32(6)−2.39(6) Å) are much longer than found in $\eta^2$-$H_2$ and related complexes.[47] This is in accord with the solution spectrocopic data (IR (benzene): $\nu$(RuH) = 1893 $cm^{-1}$; $^1H\{^{31}P\}$ NMR ($C_6D_6$): $J_{SiH}$ = 25 Hz). Evidence for nonclassical EH (E = Si or Sn) bonding, but not dihydrogen complexation, is also observed in other $L_3M(ER_3)H_3$ complexes, both in the solid state (X-ray) and in solution ($J_{EH}$ and $T_1$ relaxation times).[36,38−40]

***Table 6.*** Selected Bond Distances and Nonbonding Contacts (Å) and Angles (deg) in **4b**

| | | | | | |
|---|---|---|---|---|---|
| Ru—P1 | 2.3219(7) | Ru—H1 | 1.60(4) | Si1—H1 | 2.00(4) |
| Ru—P2 | 2.3147(7) | Ru—H2 | 1.61(3) | Si1—H2 | 2.09(4) |
| Ru—P3 | 2.3220(8) | Ru—H3 | 1.58(5) | Si1—H3 | 2.05(5) |
| H1—H2 | 2.33(5) | H2—H3 | 2.39(6) | H1—H3 | 2.32(6) |
| Ru—Si1 | 2.3774(8) | | | | |
| P1—Ru—P2 | 97.63(3) | P1—Ru—Si1 | 120.18(3) | | |
| P2—Ru—P3 | 99.86(3) | P2—Ru—Si1 | 118.99(3) | | |
| P1—Ru—P3 | 98.89(3) | P3—Ru—Si1 | 117.10(3) | | |
| Si1—Ru—H1 | 56.3(14) | P1—Ru—H1 | 176.4(14) | | |
| Si1—Ru—H2 | 59.6(13) | P1—Ru—H2 | 84.3(13) | | |
| Si1—Ru—H3 | 58(2) | P1—Ru—H3 | 84(2) | | |
| P2—Ru—H1 | 84.3(14) | P3—Ru—H1 | 83.7(14) | | |
| P2—Ru—H2 | 81.3(13) | P3—Ru—H2 | 176.4(13) | | |
| P2—Ru—H3 | 177(2) | P3—Ru—H3 | 82(2) | | |
| H1—Ru—H2 | 93(2) | H2—Ru—H3 | 97(2) | | |
| H1—Ru—H3 | 94(2) | | | | |

## Discussion

Compounds **3a**−**3c** represent an array of well-characterized models of possible structural patterns and chemical behavior of a catalytic intermediate, $(PMe_3)_3Ru(SiMe_3)_2(H)_2$ **3d**, which was long postulated in the dehydrogenative coupling of silanes but never observed prior to this work. The structure and properties of **3a**−**c** allow the spectroscopic data for **3d** to be interpreted with greater confidence. The complicated dynamic behavior and reactivity of **3d** provide insight into the catalytic dehydrocoupling process, and offers an opportunity to extract kinetic and thermodynamic information.

**Reactivity.** Compounds **3a**−**d** participate in the SiH and $H_2$ reductive eliminations. The products of these reactions, $16e^-$ intermediates, undergo a variety of oxidative processes such as SiH and $H_2$ (intermolecular) and $\beta$-CH (intramolecular) additions. The selectivity of these steps influence formation and scission of Si−C bonds, hence the efficacy of polymerization vs depolymerization and other nonproductive reactions, and bears closer examination.

The selectivity for silane or dihydrogen elimination clearly depends on the silyl substituents in **3a**−**d**. In the case of the reaction of CO with **3a** — the least hindered of the series — the activation barriers for both SiH and $H_2$ eliminations are comparable and products resulting from both processes are observed. On the other hand, the only observable products from treatment of **3b**−**3d** with CO result from silane loss, which indicates that $H_2$ elimination is at least ca. 100× slower than SiH elimination. It is likely that the primary difference between **3a** and **3b**−**d** is the greater steric congestion in the latter, which accelerates dissociation of the large silane fragment in preference to $H_2$.

The trapping experiments also reveal a clear relationship between bis(silyl) complex structure and reactivity. Thus, the

(52) Atheaux, I.; Delpech, F.; Donnadieu, B.; Sabo-Etienne, S.; Chaudret, B.; Hussein, K.; Barthelat, J. C.; Braun, T.; Duckett, S. B.; Perutz, R. N. *Organometallics* **2002**, *21*, 5347−5357.
(53) Atheaux, I.; Donnadieu, B.; Rodriguez, V.; Sabo-Etienne, S.; Chaudret, B.; Hussein, K.; Barthelat, J.-C. *J. Am. Chem. Soc.* **2000**, *122*, 5664−5665.
(54) Dubberley, S. R.; Ignatov, S. K.; Rees, N. H.; Razuvaev, A. G.; Mountford, P.; Nikonov, G. I. *J. Am. Chem. Soc.* **2003**, *125*, 642−643.

*Scheme 3*

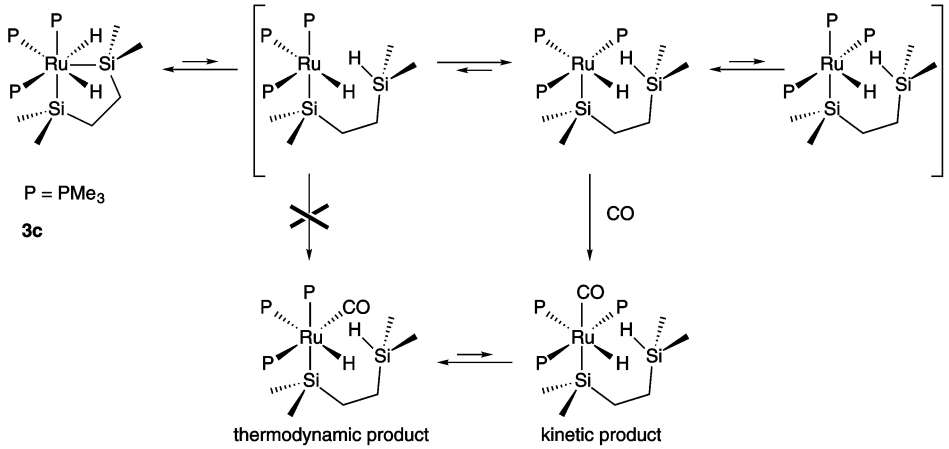


facial bis(silyl) **3c** reacts with CO orders of magnitude slower than the meridional **3a**, **3b**, and **3d**. The differences in reactivity may result from a strong trans effect of the remaining silyl and hydride ligands on the dissociating silane in **3a**, **3b**, and **3d**, whereas only weakly trans-directing phosphine ligands are trans to the silyls in **3c**.

A caveat concerning these experiments is that the geometry of the CO-trapped complexes does not necessarily reflect the geometry of the 16e$^-$ intermediate initially resulting from SiH or $H_2$ loss. It is true that the structures of *mer*-$(PMe_3)_3(CO)Ru(SiR_3)_2$ and *mer*-$(PMe_3)_3(CO)Ru(SiR_3)H$ are consistent with a loss of $H_2$ or SiH from **3a**, **3b**, and **3d** immediately followed by addition of CO to the newly formed coordination site. However, in the case of **3c** it is impossible to generate an open coordination site trans to silicon by simple Si−H dissociation without isomerization of the 16e$^-$ intermediate (Scheme 3). Clearly, addition of CO (at least in the case of **3c**) is slow relative to rearrangement of the five-coordinate species initially produced. On the basis of known analogues,[56−61] the most stable 5-coordinate intermediate should have a silyl ligand trans to the empty site (cis to hydride). Indeed, the kinetic carbonylation product of **3c** (and the other bis(silyls)) has the CO ligand trans to silyl, even though this arrangement of two strong trans-directing ligands is not thermodynamically favorable, and rearrangement to the fac-isomer is ultimately observed.

Interestingly, carbonylation of **3b** yields significant amounts (ca. 10%) of another product, *mer*-$(PMe_3)_3(CO)Ru(SiHPh_2)H$ (trans CO, H), which suggests the 16e$^-$ species with hydride trans to the empty site is fairly close in energy in this case. Thus, the trapping experiments reveal information on both the relative rates of the elimination processes in the 18e$^-$ $(PMe_3)_3Ru(SiR_3)_2(H)_2$ compounds and on the structures and relative stability of 16e$^-$ intermediates as well.

**Comparison of Inter- and Intramolecular Addition and Elimination Reactions** Bond disruption enthalpy data (BDE) are scarce for late transition metals in general and even more rare for silicon containing complexes.[21] Therefore, it is of interest to map relative thermodynamic preferences for the processes occurring in the catalytic system of **1**, **2**, and **3d**. Thermodynamic data for the SiH oxidative addition to **1** ($\Delta H_{SiH-add} = -11.0 \pm 0.6$ kcal·mol$^{-1}$; $\Delta S_{SiH-add} = -40 \pm 2$ cal·mol$^{-1}$·K$^{-1}$) can be compared against the previously reported values for $\beta$-CH activation in **1** ($\Delta H_{\beta-CH-add} = -2.7 \pm 0.3$ kcal·mol$^{-1}$; $\Delta S_{\beta-CH-add} = -6 \pm 1$ cal·mol$^{-1}$·K$^{-1}$).[5] Furthermore, qualitative thermodynamic values for the $H_2$ addition can be added to this comparison, as the products of $H_2$ addition, **4a** and **4b**, are by far more stable than those of SiH or $\beta$-CH (**3d** or **2**) at all temperatures examined. Because of the very different entropy contributions to inter- and intramolecular additions to **1**, the thermodynamic preference strongly depends on the temperature. Below ca. 250 K, the driving forces change in the following order (arranged most to least favorable): $\Delta G_{HH-add} \ll \Delta G_{SiH-add} < \Delta G_{\beta-CH-add}$. However, above ca. 250 K the preference for $\beta$-CH− over SiH activation changes: $\Delta G_{HH-add} \ll \Delta G_{\beta-CH-add} < \Delta G_{SiHadd}$. Clearly, the reactivity pattern of **1** at higher temperatures is dominated by entropic contributions and steric effects, which favor intramolecular addition of the smaller $\beta$-$CH_2$−H over intermolecular addition of $Me_3Si$−H.

It is also instructive to compare the activation parameters data for $\beta$-CH, SiH, and HH addition−elimination reactions. Unfortunately, although the former two have been measured, the $H_2$ elimination process was not directly observed in **3d** and hence could not be quantified. However, a minimum barrier for $H_2$ elimination from **3d** can be estimated. The two hydrides in **3d** are located in inequivalent, nonadjacent positions, whereas the minimal requirement for $H_2$ dissociation is a cis arrangement of the hydride ligands. The fastest dynamic process observed for **3d** that might achieve this is the intramolecular exchange of the inequivalent ruthenium hydrides, which has measured activation parameters $\Delta H^{\ddagger} = 6.5 \pm 0.6$ kcal·mol$^{-1}$ and $\Delta S^{\ddagger} = -4 \pm 2$ cal·mol$^{-1}$·K$^{-1}$. These would therefore define the *minimum* barrier for $H_2$ dissociation. In fact, this barrier most likely characterizes the partial elimination of SiH,[20,24,27,62−68] not $H_2$, and may well underestimate the barrier for $H_2$ elimina-

(55) Feldman, J. D.; Peters, J. C.; Tilley, T. D. *Organometallics* **2002**, *21*, 4065−4075.
(56) Clark, G. R.; Rickard, C. E. F.; Roper, W. R.; Salter, D. M.; Wright, L. J. *Pure Appl. Chem.* **1990**, *62*, 1039−1042.
(57) Rickard, C. E. F.; Roper, W. R.; Salter, D. M.; Wright, L. J. *Organometallics* **1992**, *11*, 3931−3933.
(58) Maddock, S. M.; Rickard, C. E. F.; Roper, W. R.; Wright, L. J. *Organometallics* **1996**, *15*, 1793−1803.
(59) Heyn, R. H.; Huffman, J. C.; Caulton, K. G. *New J. Chem.* **1993**, *17*, 797−803.
(60) Poulton, J. T.; Sigalas, M. P.; Eisenstein, O.; Caulton, K. G. *Inorg. Chem.* **1993**, *32*, 5490−5501.
(61) Huang, D.; Heyn, R. H.; Bollinger, J. C.; Caulton, K. G. *Organometallics* **1997**, *16*, 292−293.
(62) Wang, W. D.; Hommeltoft, S. I.; Eisenberg, R. *Organometallics* **1988**, *7*, 2417−2419.
(63) Wang, W. D.; Eisenberg, R. *J. Am. Chem. Soc.* **1990**, *112*, 1833−1841.

tion by a substantial margin. Even so, above 220 K, this conservative estimate for $H_2$ elimination is higher than the barrier for SiH elimination; i.e., $k_{HH-elim} \leq k_{SiH-elim}$ above 220 K.

In turning to the relative kinetic barriers for oxidative additions to **1**, it is unfortunate that activation parameters cannot be easily estimated for dihydrogen. However, the SiH addition process ($\Delta H^{\ddagger}_{SiH-add} = -1.8 \pm 0.8$ kcal·mol$^{-1}$; $\Delta S^{\ddagger}_{SiH-add} = -31 \pm 3$ cal·mol$^{-1}$·K$^{-1}$) can be compared against previously reported values for the intramolecular $\beta$-CH addition ($\Delta H^{\ddagger}_{\beta-CH-add} = 16.4 \pm 0.6$ kcal·mol$^{-1}$; $\Delta S^{\ddagger}_{\beta-CH-add} = -13 \pm 6$ cal·mol$^{-1}$·K$^{-1}$).[5] It is not surprising that the *inter*molecular addition of silane exhibits a more unfavorable entropy of activation than the *intra*molecular $\beta$-CH addition, but the difference in activation enthalpies is more interesting. The enthalpic barrier for addition of the CH bond is ca. 16 kcal·mol$^{-1}$, whereas SiH addition involves essentially no enthalpic barrier. Note that the difference in CH and SiH bond strengths is not sufficient to account for this discrepancy (100 vs ca. 95 kcal mol$^{-1}$).[69] Clearly, there is compensation of any enthalpic cost of Si−H bond weakening in the transition state by favorable SiH bond complexation. The longer bond length and greater polarizability make the SiH ideally suited for $\sigma$-bond complex formation,[33,70] and indeed, in this case the rate limiting transition state for "oxidative addition" may really be SiH coordination. On the other hand, complexation of the CH bond is not as favorable, and if occurring, does not completely compensate for CH bond weakening. Thus, despite the unfavorable activation entropy for silane addition to **1**, CH addition is slower at all reasonable reaction temperatures (< ca. 350 °C).

## Conclusions

Bis(silyl) dihydride complexes $(PMe_3)_3Ru(SiR_3)_2(H)_2$ ($(SiR_3)_2 = (SiH_2Ph)_2$, **3a**, $(SiHPh_2)_2$, **3b**, and $(SiMe_2CH_2CH_2SiMe_2)$, **3c**) are stable and exhibit pentagonal bipyramidal geometries. A meridional arrangement of the three phosphines is generally preferred, except in the case of the chelating bis(silyl) **3c**. Although there is no evidence for nonclassical Si−H interactions in **3a** and **b**, the equatorial silyl group in **3c** is in close contact with one hydride (1.81(4) Å) and is moderately close to the other hydride (2.15(3) Å) in the solid state and solution ($\nu$(Ru···H···Si) = 1740 cm$^{-1}$ and $\nu$(RuH) = 1940 cm$^{-1}$). The highly hindered bis(trimethylsilyl) analogue, $(PMe_3)_3Ru(SiMe_3)_2(H)_2$ (**3d**), an intermediate postulated in catalytic C−H bond activation/functionalization processes, is not stable above ca. −30 °C, but can be characterized spectroscopically at low temperatures. The structure of **3d** in solution is similar to that of **3a** and **3b**. Treatment of **1** with $HSiMe_3$ at room temperature leads to formation of $(PMe_3)_3Ru(SiMe_2CH_2SiMe_3)H_3$ (**4b**), the CH functionalization process critical to catalytic dehydrocoupling of $HSiMe_3$ at higher temperatures. Closer inspection of this reaction between −110 and −10 °C by NMR reveals a plethora of silyl hydride phosphine complexes formed by ligand redistribution prior to CH activation. Following silane dehydrogenation above ca. 0 °C, this array of complexes evolves into a very simple mixture of the very stable tris(phosphine) trihydride silyls **4a** and **4b**. The key CH cleavage and SiC formation steps almost certainly proceed via $\beta$-H elimination from some manner of $L_nRu(SiMe_3)_2$ complex; however, it is clear that the exact number and arrangement of co-ligands cannot be specified in this system.

The least hindered complex, **3a**, reacts with carbon monoxide principally via an $H_2$ elimination pathway, with SiH elimination as a minor process. However, only SiH elimination is observed for **3b**−**d**. This suggests that $H_2$ elimination — a critical step in any dehydrogenative coupling process — is thermodynamically and kinetically viable in the presence of silyl ligands, but that steric crowding increases the preference for loss of the larger silane molecule. The reaction of **3c** with carbon monoxide is orders of magnitude slower than **3a**, **3b**, or **3d**, reflecting the different geometry of the chelated complex and the resultant lack of strong labilizing ligands trans to the silyl groups.

The most hindered bis(silyl) complex, **3d**, is extremely labile and even in the absence of CO undergoes SiH reductive elimination to generate the 16e$^-$ species **1**. This process is reversible and fast on the NMR time scale above 173 K, allowing to quantify thermodynamic and kinetic parameters for silane elimination ($\Delta H_{SiH-elim} = 11.0 \pm 0.6$ kcal·mol$^{-1}$ and $\Delta S_{SiH-elim} = 40 \pm 2$ cal·mol$^{-1}$·K$^{-1}$; $\Delta H^{\ddagger}_{SiH-elim} = 9.2 \pm 0.8$ kcal·mol$^{-1}$ and $\Delta S^{\ddagger}_{SiH-elim} = 9 \pm 3$ cal·mol$^{-1}$·K$^{-1}$). Reductive elimination of $H_2$ cannot be quantified at low temperatures, but is clearly a minor process. The *minimum* barrier for $H_2$ elimination, estimated based on the intramolecular rearrangement of **3d** required to place the two hydrides cis, is higher than the barrier for silane elimination at all temperatures above ca. 220 K.

The thermodynamic preferences for oxidative additions to **1** are dominated by entropy contributions and steric effects. Addition of $H_2$ is by far most favorable, whereas the relative aptitudes for intramolecular $\beta$-CH[5] and intermolecular SiH addition are strongly dependent on temperature ($\Delta H_{SiH-add} = -11.0 \pm 0.6$ kcal·mol$^{-1}$ and $\Delta S_{SiH-add} = -40 \pm 2$ cal·mol$^{-1}$·K$^{-1}$; $\Delta H_{\beta-CH-add} = -2.7 \pm 0.3$ kcal·mol$^{-1}$ and $\Delta S_{\beta-CH-add} = -6 \pm 1$ cal·mol$^{-1}$·K$^{-1}$). Thus, SiH addition is favored below ca. 250 K, whereas $\beta$-CH addition is preferred at higher temperatures. The kinetic parameters for intramolecular CH[5] and intermolecular SiH oxidative addition to **1** are as follows: $\Delta H^{\ddagger}_{SiH-add} = -1.8 \pm 0.8$ kcal·mol$^{-1}$ and $\Delta S^{\ddagger}_{SiH-add} = -31 \pm 3$ cal·mol$^{-1}$·K$^{-1}$; $\Delta H^{\ddagger}_{\beta-CH-add} = 16.4 \pm 0.6$ kcal·mol$^{-1}$ and $\Delta S^{\ddagger}_{\beta-CH-add} = -13 \pm 6$ cal·mol$^{-1}$·K$^{-1}$. The relative enthalpies of activation are particularly instructive and are interpreted in terms of strong SiH $\sigma$-complex formation — and much weaker CH coordination — in the transition state for oxidative addition.

## Experimental Section

All manipulations were performed in Schlenk-type glassware on a dual-manifold Schlenk line or in a nitrogen-filled Vacuum Atmospheres glovebox. NMR spectra were obtained at 200- and 500-MHz (for $^1$H) on Bruker AF-200 and AM-500 FT NMR spectrometers, respectively. All NMR spectra were recorded at 303 K unless stated otherwise. Chemical shifts are reported relative to tetramethylsilane for $^1$H, $^{13}$C,

(64) Fryzuk, M. D.; Rosenberg, L.; Rettig, S. J. *Inorg. Chim. Acta* **1994**, *222*, 345−364.
(65) Sun, J.; Lu, R. S.; Bau, R.; Yang, G. K. *Organometallics* **1994**, *13*, 1317−1325.
(66) Fryzuk, M. D.; Rosenberg, L.; Rettig, S. J. *Organometallics* **1996**, *15*, 2871−2880.
(67) Buil, M. L.; Espinet, P.; Esteruelas, M. A.; Lahoz, F. J.; Lledos, A.; Martinez-Ilarduya, J. M.; Maseras, F.; Modrego, J.; Onate, E.; Oro, L. A.; Sola, E.; Valero, C. *Inorg. Chem.* **1996**, *35*, 1250−1256.
(68) Butts, M. D.; Bryan, J. C.; Luo, X.-L.; Kubas, G. J. *Inorg. Chem.* **1997**, *36*, 3341−3353.
(69) Becerra, R.; Walsh, R. In *The Chemistry of Organic Silicon Compounds*; Rappoport, Z., Apeloig, Y., Eds.; John Wiley & Sons Ltd.: New York, 1998; Vol. 2, pp 154−180.
(70) Rabaa, H.; Saillard, J. Y.; Schubert, U. *J. Organomet. Chem.* **1987**, *330*, 397−413.

and $^{29}$Si spectra, and external 85% $H_3PO_4$ for $^{31}$P resonances. $^{13}$C and $^{31}$P NMR spectra were recorded with broadband $^1$H decoupling. $^{29}$Si NMR spectra were obtained using a DEPT-135 pulse sequence with $^1$H refocusing. Infrared spectra were recorded on a Perkin-Elmer Model 1430 spectrometer. HRMS were acquired on a AutoSpec (Micromass) with chemical ionization ($CH_4$). Elemental analyses were performed by Robertson Laboratory, Inc. (Madison, NJ).

Hydrocarbon solvents were dried over Na/K alloy-benzophenone. Benzene-$d_6$, cyclohexane-$d_{12}$, and methylcyclohexane-$d_{14}$ were dried over Na/K alloy. Trimethylsilane was prepared by the reaction of $Me_3SiCl$ and $LiAlH_4$ in $^nBu_2O$, and purified by trap-to-trap vacuum fractionation. $H_2$ and CO (Airco) were used as received. $(PMe_3)_4RuH_2$,[42] $(PMe_3)_3Ru(SiMe_3)H_3$,[42] $(PMe_3)_4Ru(SiMe_3)H$,[42] $PhSiH_3$,[71] and $PMe_3$[72] were synthesized according to the literature procedures.

NMR samples were prepared in an NMR assembly consisting of an NMR tube and a side bulb fused to a Teflon stopcock and a ground glass joint. Simulations of the dynamic NMR spectra were carried out using gNMR software package (v3.6 for Macintosh, Cherwell Scientific Publishing Limited). The rates of exchange as a function of temperature were determined from visual comparison of the experimental and simulated spectra. The errors in the rate constants of ca. 10% were estimated on the basis of subjective judgments of the sensitivity of the fits to changes in the rate constants. The equilibrium concentrations in the fast exchange regime were determined by fitting the experimental chemical shifts to the weighted average of the known shifts of components determined in the slow exchange regime. The temperature of the NMR probe was calibrated against methanol (estimated error 0.3 K). The activation parameters were calculated from the Eyring equation by using a linear least-squares procedure, and the errors were computed from error propagation formulas.[73]

**Synthesis of $(PMe_3)_3Ru(SiH_2Ph)_2(H)_2$.** A solution of $(PMe_3)_3Ru(SiMe_3)H_3$ (508 mg, 1.25 mmol) and $PhSiH_3$ (620 mg, 5.75 mmol) in *n*-pentane (3 mL) was stirred for 17 h at RT. $(PMe_3)_3Ru(SiH_2Ph)_2(H)_2$ precipitated as pale yellow crystals. Yield 580 mg (83%).

$(PMe_3)_3Ru(SiH_2Ph)_2(H)_2$: $^1$H NMR ($C_6D_6$) $\delta$ −8.00 (br s, 2H, Ru*H*), 1.06 (s, 18H, *axial*-P*Me*$_3$), 1.13 (d, $J_{PH}$ = 7.0 Hz, 9H, *equatorial*-P*Me*$_3$), 5.18 (br q, $J_{PH}$ = 9.0 Hz, 4H, Si*H*$_2$), 7.22 (t, $J_{HH}$ = 7.0 Hz, 2H, *p*-*H*-Ph), 7.35 (m, $J_{HH}$ = 7.0 Hz, 4H, *m*-*H*-Ph), 8.18 (dd, $J_{HH}$ = 6.8 and 1.0 Hz, 4H, *o*-*H*-Ph); $^1$H NMR (toluene-$d_8$, 225 K) $\delta$ −9.20 (dt, $J_{PH}$ = 44 and 18 Hz, 1H, Ru*H*), −6.95 (dm, $J_{PH}$ = 34 Hz, 1H, Ru*H*), 1.03 (t, $J_{PH}$ = 2.6 Hz, 18H, *axial*-P*Me*$_3$), 1.07 (d, $J_{PH}$ = 7.0 Hz, 9H, *equatorial*-P*Me*$_3$), 4.81 (br q, $J_{PH}$ = 9.5 Hz, 2H, Si*H*$_2$), 5.57 (sept, $J_{PH}$ = 5 Hz, 2H, Si*H*$_2$), 7.23 (t, $J_{HH}$ = 7.0 Hz, 1H, *p*-*H*-Ph), 7.27 (t, $J_{HH}$ = 7.0 Hz, 1H, *p*-*H*-Ph), 7.35 (t, $J_{HH}$ = 7.0 Hz, 2H, *m*-*H*-Ph), 7.40 (t, $J_{HH}$ = 7.0 Hz, 2H, *m*-*H*-Ph), 8.20 (d, $J_{HH}$ = 7 Hz, 2H, *o*-*H*-Ph), 8.23 (d, $J_{HH}$ = 7 Hz, 2H, *o*-*H*-Ph); $^{13}$C{$^1$H} NMR (thf-$d_8$) $\delta$ 21.6 (t, $J_{PC}$ = 17 Hz, *axial*-P*Me*$_3$), 24.3 (d, $J_{PC}$ = 27 Hz, *equatorial*-P*Me*$_3$), 127.6 (s, *p*-*C*-Ph), 127.8 (s, *m*-*C*-Ph), 136.6 (s, *o*-*C*-Ph), 146.1 (s, *ipso*-*C*-Ph); $^{29}$Si NMR ($C_6D_6$) $\delta$ −15.8 (br s); $^{31}$P NMR ($C_6D_6$) $\delta$ −15.2 (t, $J_{PP}$ = 32.4 Hz, 1P, *equatorial*-*P*Me$_3$), −5.9 (d, $J_{PP}$ = 32.4 Hz, 2P, *axial*-*P*Me$_3$). IR (benzene) $\nu$(SiH) = 2033, 2010 cm$^{-1}$, $\nu$(RuH) = 1953 and 1864 cm$^{-1}$; (Nujol) $\nu$(SiH) = 2031, 2006 cm$^{-1}$, $\nu$(RuH) = 1952 and 1861 cm$^{-1}$, HRMS (CI) Calcd 544.1003 (M($^{102}$Ru)-2H)$^+$, Found 544.0989, Calcd 546.1014 (M($^{104}$Ru)-2H)$^+$, Found 546.1008.

**Synthesis of $(PMe_3)_3Ru(SiHPh_2)_2(H)_2$.** A solution of $(PMe_3)_3Ru(SiMe_3)H_3$ (200 mg, 0.49 mmol) and $Ph_2SiH_2$ (360 mg, 1.96 mmol) in toluene (1 mL) was stirred for 3 days at RT. $(PMe_3)_3Ru(SiHPh_2)_2(H)_2$ precipitated as colorless crystals. Yield 290 mg (85%). Compound **3b** can also be prepared by the reaction of $PMe_3)_4Ru(H)Me$ with excess $Ph_2SiH_2$ (benzene solution, 12 h reflux).

$(PMe_3)_3Ru(SiHPh_2)_2(H)_2$: $^1$H NMR ($C_6D_6$) $\delta$ −7.71 (br s, 2H, Ru*H*), 0.82 (t, $J_{PH}$ = 2.6 Hz, 18H, *axial*-P*Me*$_3$), 1.22 (d, $J_{PH}$ = 6.8 Hz, 9H, *equatorial*-P*Me*$_3$), 5.84 (br s, 2H, Si*H*), 7.16 (t, $J_{HH}$ = 6.8 Hz, 4H, *p*-*H*-Ph), 7.29 (t, $J_{HH}$ = 7.0 Hz, 8H, *m*-*H*-Ph), 8.06 (dd, $J_{HH}$ = 7.0 and 1.2 Hz, 8H, *o*-*H*-Ph); $^1$H NMR (toluene-$d_8$, 225 K) $\delta$ −8.34 (dt, $J_{PH}$ = 47 and 17 Hz, 1H, Ru*H*), −7.13 (dt, $J_{PH}$ = 33 and 15 Hz, 1H, Ru*H*), 0.74 (m, 18H, *axial*-P*Me*$_3$), 1.15 (m, 9H, *equatorial*-P*Me*$_3$), 5.66 (dt, $J_{PH}$ = 16 and 6 Hz, 1H, Si*H*), 6.19 (t, $J_{PH}$ = 8 Hz, 1H, Si*H*), 7.16 (t, $J_{HH}$ = 7.5 Hz, 2H, *p*-*H*-Ph), 7.24 (t, $J_{HH}$ = 7.5 Hz, 2H, *p*-*H*-Ph), 7.27 (t, $J_{HH}$ = 7.5 Hz, 4H, *m*-*H*-Ph), 7.37 (t, $J_{HH}$ = 7.5 Hz, 4H, *m*-*H*-Ph), 8.09 (d, $J_{HH}$ = 7.5 Hz, 4H, *o*-*H*-Ph), 8.11 (d, $J_{HH}$ = 7.5 Hz, 4H, *o*-*H*-Ph); $^{13}$C{$^1$H} NMR (thf-$d_8$) $\delta$ 22.4 (dt, $J_{PC}$ = 3.0 and 15.0 Hz, *axial*-P*Me*$_3$), 25.1 (td, $J_{PC}$ =3 and 25 Hz, *equatorial*-P*Me*$_3$), 127.5 (s, *p*-*C*-Ph), 127.7 (s, *m*-*C*-Ph), 137.2 (t, $J_{PC}$ = 9.0 Hz, *o*-*C*-Ph), 148.5 (br s, *ipso*-*C*-Ph); $^{31}$P NMR (thf-$d_8$) $\delta$ −17.0 (t, $J_{PP}$ = 34 Hz, 1P, *equatorial*-*P*Me$_3$), −9.54 (d, $J_{PP}$ = 34 Hz, 2P, *axial*-*P*Me$_3$). IR (Nujol) $\nu$(SiH) = 2083, 2014 cm$^{-1}$, $\nu$(RuH) = 1956 and 1900 cm$^{-1}$. Elemental analysis: found (calculated) C 56.67 (56.79), H 7.34 (7.37).

**Observation of $(PMe_3)_3Ru(SiHPh_2)H_3$.** A solution of $(PMe_3)_3Ru(SiMe_3)H_3$ (21 mg, 0.05 mmol) and $Ph_2SiH_2$ (15 mg, 0.08 mmol) in $C_6D_6$ (0.36 mL) was kept for 18 h at RT. The product ratio was estimated by $^1$H NMR to be 10% of $(PMe_3)_3Ru(SiHPh_2)_2(H)_2$ and 90% of $(PMe_3)_3Ru(SiHPh_2)H_3$.

$(PMe_3)_3Ru(SiHPh_2)H_3$: $^1$H NMR ($C_6D_6$) $\delta$ −9.71 (s, 3H, Ru*H*), 1.05 (dd $J$ = 2.4 and 2.7 Hz, 27H, P*Me*$_3$), 6.58 (m, $J_{PH}$ = 2.7 Hz, 1H, Si*H*), 7.19 (t, $J_{HH}$ = 7.0 Hz, 2H, *p*-*H*-Ph), 7.30 (t, $J_{HH}$ = 7.0 Hz, 4H, *m*-*H*-Ph), 8.05 (dd, $J_{HH}$ = 7.8 and 1.2 Hz, 4H, *o*-*H*-Ph).

**$(PMe_3)_3Ru(SiMe_2CH_2SiMe_3)H_3$ (4b).** A hexanes solution (10 mL) of $(PMe_3)_3Ru(SiMe_3)H_3$ (81 mg, 0.2 mmol) and $HSiMe_2CH_2SiMe_3$ (146 mg, 1.0 mmol) was stirred for 1 h at 70 °C, degassed for 5 min at −40 °C to remove $HSiMe_3$, and stirred for another hour at 70 °C. Volatiles were removed in vacuo to yield spectroscopically pure **4b** in essentially quantitative yield. Recrystallization from petroleum ether affords analytically pure crystals. Anal. Calcd. for $C_{15}H_{47}P_3Si_2Ru$: C, 37.72; H, 9.92. Found: C, 37.77; H, 10.47. $^1$H NMR ($C_6D_6$) $\delta$ 1.14 (m, 27H, P*Me*$_3$), 0.92 (s, 6H, Si*Me*$_2$), 0.58 (s, 2H, C*H*$_2$), 0.38 (s, 9H, Si*Me*$_3$), −10.15 (br m, 3H, Ru*H*$_3$); $^1$H{$^{31}$P} NMR ($C_6D_6$) $\delta$ −10.15 (s, 3H, $J_{HSi}$ = 25 Hz, Ru*H*$_3$); $^1$H NMR ($C_6D_{12}$) $\delta$ 1.34 (m, 27H, P*Me*$_3$), 0.40 (s, 6H, Si*Me*$_2$), 0.16 (s, 2H, C*H*$_2$), 0.02 (s, 9H, Si*Me*$_3$), −10.27 (br m, 3H, Ru*H*$_3$); $^{13}$C{$^1$H} NMR ($C_6D_6$) $\delta$ 26.6 (m, P*Me*$_3$), 22.3 (d, $^3J_{PC}$ = 2.7 Hz, *C*H$_2$), 20.2 (d, $^3J_{PC}$ = 3.5 Hz, Si*Me*$_2$), 2.7 (s, $J_{SiC}$ = 50.4 Hz, Si*Me*$_3$); $^{29}$Si NMR ($C_6D_6$) $\delta$ −0.9 (s, *Si*Me$_3$), −9.2 (q, $^2J_{PSi}$ = 7.7 Hz, *Si*Me$_2$); $^{31}$P{$^1$H} NMR ($C_6D_6$) $\delta$ −5.3 (s, *P*Me$_3$). IR (Nujol): $\nu$(RuH) = 1898 cm$^{-1}$. IR (benzene): $\nu$(RuH) = 1893 cm$^{-1}$.

**Synthesis of *mer*-$(PMe_3)_3(CO)Ru(SiH_2Ph)_2$.** A solution of $(PMe_3)_3Ru(SiH_2Ph)_2(H)_2$ (60 mg, 0.11 mmol) in benzene (2 mL) was stirred for 17 h at RT under 1 atm of CO. The volatiles were removed under vacuum, and the residue was recrystallized from $Et_2O$ to yield 40 mg (64%) of colorless *mer*-$(PMe_3)_3(CO)Ru(SiH_2Ph)_2$.

*mer*-$(PMe_3)_3(CO)Ru(SiH_2Ph)_2$: $^1$H NMR ($C_6D_6$) $\delta$ 1.09 (d, $J_{PH}$ = 6.2 Hz, 9H, P*Me*$_3$), 1.10 (t, $J_{PH}$ = 3.1 Hz, 18H, mutually *trans*-P*Me*$_3$), 4.51 (dt, $J_{PH}$ = 7.0 and 14.0 Hz, 2H, Si*H*$_2$), 4.83 (dt, $J_{PH}$ = 6.2 and 11.0 Hz, 2H, Si*H*$_2$), 7.22 (t, $J_{HH}$ = 6.2 Hz, 4H, *m*-*H*-Ph), 7.34 (t, $J_{HH}$ = 7.3 Hz, 2H, *p*-*H*-Ph), 7.98 (dd, $J_{HH}$ = 7.2 and 1.4 Hz, 2H, *o*-*H*-Ph) and 8.23 (dd, $J_{HH}$ = 7.0 and 1.4 Hz, 2H, *o*-*H*-Ph); $^{13}$C{$^1$H} NMR (thf-$d_8$) $\delta$ 21.56 (dt, $J_{PC}$ = 4 and 16 Hz, mutually *trans*-P*Me*$_3$), 22.49 (td, $J_{PC}$ = 2 and 23 Hz, P*Me*$_3$), 127.20 (s, *p*-*C*-Ph), 127.22 (s, *p*-*C*-Ph), 127.46 (s, *m*-*C*-Ph), 127.56 (s, *m*-*C*-Ph), 137.13 (s, *o*-*C*-Ph), 145.89 (d, $J_{PC}$ = 2 Hz, *ipso*-*C*-Ph), 146.55 (d, $J_{PC}$ = 2 Hz, *ipso*-*C*-Ph) and 204.95 (dt, $J_{PC}$ = 9 and 14 Hz, *C*O); $^{29}$Si NMR (thf-$d_8$) $\delta$ −20.1 (q, $J_{SiP}$ = 22.1 Hz, *Si* trans to CO), −11.9 (dt, $J_{SiP}$ = 84.3 and 13.3 Hz, *Si* trans to P); $^{31}$P NMR (thf-$d_8$) $\delta$ −23.45 (t, $J_{PP}$ = 28 Hz, 1P, *P*Me$_3$), −13.73 (d, $J_{PP}$ = 28 Hz, 2P, mutually *trans*-*P*Me$_3$); $^{31}$P NMR ($C_6D_6$) $\delta$ −22.2 (t, $J_{PP}$ = 27 Hz, 1P, *P*Me$_3$), −12.5 (d, $J_{PP}$ = 27 Hz, 2P, mutually *trans*-*P*Me$_3$). IR (film casted from solution in THF) $\nu$(SiH)

(71) Finholt, A. E.; Bond, A. C. J.; Wilzbach, K. E.; Schlesinger, H. I. *J. Am. Chem. Soc.* **1947**, *69*, 2692−2696.
(72) Luetkens, M. L.; Sattelberger, A. P.; Murray, H. H.; Basil, J. D.; Fackler, J. P. *Inorg. Synth.* **1989**, *26*, 7.
(73) Morse, P. M.; Spencer, M. D.; Wilson, S. R.; Girolami, G. S. *Organometallics* **1994**, *13*, 1646−1655.

= 2022, 2005 $cm^{-1}$, $\nu$(CO) = 1915 $cm^{-1}$, HRMS (CI) Calcd 571.0874 $(M-H)^+$, Found 571.0835.

**Reaction of $(PMe_3)_3Ru(SiH_2Ph)_2(H)_2$ with CO.** An NMR sample of $(PMe_3)_3Ru(SiH_2Ph)_2(H)_2$ (6 mg, 0.011 mmol) in $C_6D_6$ (0.4 mL) was flame sealed under 1 atm of CO. After 3 days at RT the product ratio was estimated by $^1H$ NMR to be 15% of *mer*-$(PMe_3)_3(CO)Ru(SiH_2Ph)H$, 65% of *mer*-$(PMe_3)_3(CO)Ru(SiH_2Ph)_2$, and 20% of $(PMe_3)_2(CO)_2Ru(SiH_2Ph)_2$. After 11 days at RT the product ratio changed to 15:35:50%, respectively.

$(PMe_3)_2(CO)_2Ru(SiH_2Ph)_2$: $^1H$ NMR ($C_6D_6$) $\delta$ 1.08 (t, $J_{PH}$ = 3.6 Hz, 18H, mutually *trans*-P*Me*$_3$), 4.58 (t, $J_{PH}$ = 9.3 Hz, 4H, Si*H*$_2$), 7.3 (m, 6H, *m*- and *p*-*H*-Ph), 7.89 (dd, $J_{HH}$ = 7.8 and 1.4 Hz, 4H, *o*-*H*-Ph); $^{13}C\{^1H\}$ NMR (thf-$d_8$) $\delta$ 19.9 (t, $J_{PC}$ = 17.5 Hz, mutually *trans*-P*Me*$_3$), 128.05 and 128.9 (s, *p*- and *m*-*C*-Ph), 136.2 (s, *o*-*C*-Ph), 144.0 (t, $J_{PC}$ = 1.6 Hz, *ipso*-*C*-Ph) and 201.1 (t, $J_{PC}$ = 13 Hz, *C*O); $^{29}Si$ NMR (thf-$d_8$) $\delta$ −16.0 (t, $J_{SiP}$ = 20.2 Hz, 2Si, *Si* trans to CO); $^{29}Si$ NMR ($C_6D_6$) $\delta$ −15.4 (t, $J_{SiP}$ = 20.0 Hz, 2Si, *Si* trans to CO); $^{31}P$ NMR (thf-$d_8$) $\delta$ −16.5 (s, 2P, mutually *trans*-*P*Me$_3$); $^{31}P$ NMR ($C_6D_6$) $\delta$ −15.4 (s, 2P, mutually *trans*-*P*Me$_3$);.

*mer*-$(PMe_3)_3(CO)Ru(SiH_2Ph)H$: $^1H$ NMR ($C_6D_6$) $\delta$ −8.72 (dt, $J_{PH}$ = 68 and 27 Hz, 1H, RuH), 0.87 (d, $J_{PH}$ = 8.0 Hz, 9H, P*Me*$_3$), 1.20 (t, $J_{PH}$ = 2.8 Hz, 18H, mutually *trans*-P*Me*$_3$), 4.86 (m, $J_{PH}$ = 7.6 Hz, 2H, Si*H*$_2$), 7.2−7.3 (m, 3H, *m*- and *p*-*H*-Ph), 8.30 (d, $J_{HH}$ = 7.8 Hz, 2H, *o*-*H*-Ph); $^{13}C\{^1H\}$ NMR (thf-$d_8$) $\delta$ 20.95 (dt, $J_{PC}$ = 4 and 16 Hz, mutually *trans*-P*Me*$_3$), 22.9 (td, $J_{PC}$ = 3 and 22 Hz, P*Me*$_3$), 128.9 and 130.7 (s, *m*- and *p*-*C*-Ph), 136.4 (s, *o*-*C*-Ph), 145.8 (m, *ipso*-*C*-Ph), 202.6 (m, *C*O).

**Reaction of $(PMe_3)_3Ru(SiHPh_2)_2(H)_2$ with CO.** An NMR sample of $(PMe_3)_3Ru(SiHPh_2)_2(H)_2$ (6 mg, 0.01 mmol) in $C_6D_6$ (0.5 mL) was flame sealed under 1 atm of CO. After 10 min at RT the product ratio was estimated by $^1H$ NMR to be 80% of *mer*-$(PMe_3)_3(CO)Ru(SiHPh_2)H$ (trans CO, Si), 14% of *fac*-$(PMe_3)_3(CO)Ru(SiHPh_2)H$ and 6% of *mer*-$(PMe_3)_3(CO)Ru(SiHPh_2)H$ (trans CO, H). After 1 h at RT the product ratio changed to 40:50:10%, respectively. IR bands of the three isomers are not resolved: ($C_6D_6$) $\nu$(SiH) = 2010 $cm^{-1}$, $\nu$(CO) = 1920 $cm^{-1}$. The following spectral data were determined from the mixture of isomers:

*mer*-$(PMe_3)_3(CO)Ru(SiHPh_2)H$ (trans CO, Si): $^1H$ NMR ($C_6D_6$) $\delta$ −8.66 (dt, $J_{PH}$ = 71.9 and 25.6 Hz, 1H, RuH), 1.09 (d, $J_{PH}$ = 5.9 Hz, 9H, P*Me*$_3$), 1.12 (t, $J_{PH}$ = 3.4 Hz, 18H, mutually *trans*-P*Me*$_3$), 5.41 (q, $J_{PH}$ = 10.5 Hz, 1H, Si*H*), 7.25 (t, $J_{HH}$ = 7.4 Hz, 4H, *m*-*H*-Ph), 7.32 (quintet, $J_{HH}$ = 7.4 Hz, 2H *p*-*H*-Ph), 8.00 (dd, $J_{HH}$ = 2.0 and 7.9 Hz, 4H, *o*-*H*-Ph); $^{31}P$ NMR ($C_6D_6$) $\delta$ −19.0 (m, 1P, *P*Me$_3$), −7.56 (d, $J_{PP}$ = 23.3 Hz, 2P, mutually *trans*-*P*Me$_3$).

*fac*-$(PMe_3)_3(CO)Ru(SiHPh_2)H$: $^1H$ NMR ($C_6D_6$) $\delta$ −8.80 (ddd, $J_{PH}$ = 66.3, 28.4 and 22.1 Hz, 1H, RuH), 0.97 (d, $J_{PH}$ = 5.9 Hz, 9H, P*Me*$_3$), 1.01 (d, $J_{PH}$ = 6.9 Hz, 9H, P*Me*$_3$), 1.10 (d, $J_{PH}$ = 6.9 Hz, 9H, P*Me*$_3$), 5.53 (ddd, $J_{PH}$ = 5.3, 6.3 and 16.9 Hz, 1H, Si*H*), 7.25−7.35 (m, 6H, *p*- *and m*-*H*-Ph), 8.09 (dd, $J_{HH}$ = 2.0 and 7.9 Hz, 2H, *o*-*H*-Ph), 8.38 (dd, $J_{HH}$ = 2.0 and 7.9 Hz, 2H, *o*-*H*-Ph); $^{31}P$ NMR ($C_6D_6$) $\delta$ −19.6 (dd, $J_{PP}$ = 21.5 and 37.0 Hz, 1P, *P*Me$_3$), −18.6 (m, 1P, *P*Me$_3$), −13.2 (t, $J_{PP}$ = 21.5 and 37.0 Hz, 1P, *P*Me$_3$).

*mer*-$(PMe_3)_3(CO)Ru(SiHPh_2)H$ (trans CO, H): $^1H$ NMR ($C_6D_6$) $\delta$ −7.93 (ddt, $J_{HH}$ = 5.2 Hz, $J_{PH}$ = 17.9 and 29.8 Hz, 1H, RuH), 1.07 (t, $J_{PH}$ = 3.0 Hz, 18H, mutually *trans*-P*Me*$_3$), 1.09 (d, $J_{PH}$ = 7.5 Hz, 9H, P*Me*$_3$), 5.75 (ddt, $J_{HH}$ = 5.6 Hz, $J_{PH}$ = 5.6 and 16.2 Hz, 1H, Si*H*), 7.2−7.3 (m, 6H, *p*- *and m*-*H*-Ph), 8.14 (d, $J_{HH}$ = 7.4 Hz, 4H, *o*-*H*-Ph); $^{31}P$ NMR ($C_6D_6$) $\delta$ −2.1 (d, $J_{PP}$ = 30.5 Hz, 2P, mutually *trans*-*P*Me$_3$), −14.8 (t, $J_{PP}$ = 30.5 Hz, 1P, *P*Me$_3$), HRMS (CI) Calcd 541.0948 $(M-H)^+$, Found 541.0947.

**Reaction of $(PMe_3)_3Ru(SiHPh_2)_2(H)_2$ with $PMe_3$.** $(PMe_3)_3Ru(SiHPh_2)_2(H)_2$ (7 mg, 0.01 mmol) was mixed with $PMe_3$ (0.23 mmol) in $C_6D_6$ (0.4 mL) and kept for 15 min at RT. A $^1H$ NMR spectrum showed a 100% conversion to $(PMe_3)_4Ru(SiHPh_2)H$.

$(PMe_3)_4Ru(SiHPh_2)H$: $^1H$ NMR ($C_6D_6$) $\delta$ −10.52 (m, 1H, RuH), 1.13 (d, $J_{PH}$ = 5.4 Hz, 18H, mutually *cis*-P*Me*$_3$), 1.19 (t, $J_{PH}$ = 2.6 Hz, 18H, mutually *trans*-P*Me*$_3$), 5.71 (tt, $J_{PH}$ = 13.8 and 4.4 Hz, 1H, Si*H*), 7.19 (t, $J_{HH}$ = 7.0 Hz, 2H, *p*-*H*-Ph), 7.31 (t, $J_{HH}$ = 7.0 Hz, 4H, *m*-*H*-Ph), 8.12 (d, $J_{HH}$ = 6.8 Hz, 4H, *o*-*H*-Ph).

**Synthesis of $(PMe_3)_3Ru(SiMe_2CH_2CH_2SiMe_2)(H)_2$.** A solution of $(PMe_3)_4Ru(H)SiMe_3$ (398 mg, 0.83 mmol) and $HSiMe_2CH_2CH_2SiMe_2H$ (146 mg, 1.0 mmol) in toluene (5 mL) was stirred for 10 min at RT, cooled to −25 °C, and the volatiles were slowly removed in vacuo. The residue was recrystallized from a mixture of *n*-pentane and toluene (3:1) to furnish a colorless crystalline $(PMe_3)_3Ru(SiMe_2CH_2CH_2SiMe_2)(H)_2$. Yield 340 mg (85%).

$(PMe_3)_3Ru(SiMe_2CH_2CH_2SiMe_2)(H)_2$: $^1H$ NMR (toluene-$d_8$) $\delta$ −10.37 (s, 2H, Ru*H*), 0.53 (s, 12H, Si*Me*$_2$), 1.00 (s, 4H, C*H*$_2$), 1.15 (t, $J_{PH}$ = 2.3 Hz, 27H, P*Me*$_3$); $^1H\{^{31}P\}$ NMR (toluene-$d_8$) $\delta$ −10.37 (s, 2H, $J_{HSi}$ = 16 Hz, Ru*H*); (methylcyclohexane-$d_{14}$, 150 K) −10.53 (s, 2H, Ru*H*), 0.07 (s, 12H, Si*Me*$_2$), 0.38 (br s, 4H, C*H*$_2$), 1.16 (br s, 27H, P*Me*$_3$); $^{13}C$ NMR (toluene-$d_8$) $\delta$ 12.63 (qq, $J_{PC}$ = 3.4 and 116.6 Hz, Si*Me*$_2$), 21.71 (qq, $J_{PC}$ = 2.6 and 119.2 Hz, *C*H$_2$), 26.36 (mq, $J_{PC}$ = 128.1 Hz, P*Me*$_3$); $^{29}Si$ NMR (toluene-$d_8$) $\delta$ −19.29 (q, $J_{PSi}$ = 13.4 Hz, *Si*Me$_2$); $^{31}P$ NMR (toluene-$d_8$) $\delta$ −13.29 (s, *P*Me$_3$); (methylcyclohexane-$d_{14}$, 180 K) −11.49 (s, *P*Me$_3$). IR (Nujol) $\nu$(Ru···H···Si) = 1740 $cm^{-1}$, $\nu$(RuH) = 1940 $cm^{-1}$. Elemental analysis: Found (Calculated) C 36.57 (37.87), H 9.25 (9.53), HRMS (CI) Calcd 476.1316 $(M(^{102}Ru))^+$, Found 476.1265; Calcd 478.1334 $(M(^{104}Ru))^+$, Found 478.1292.

**Reaction of $(PMe_3)_3Ru(SiMe_2CH_2CH_2SiMe_2)(H)_2$ with CO.** An NMR sample of $(PMe_3)_3Ru(SiMe_2CH_2CH_2SiMe_2)(H)_2$ (10 mg, 0.02 mmol) in $C_6D_6$ (0.5 mL) was flame sealed under 1 atm of CO. After 10 min at RT, the only product is *mer*-$(PMe_3)_3(CO)Ru(SiMe_2CH_2CH_2SiMe_2H)H$ (10%). After 24 h at RT, the product ratio is 96% *fac*-$(PMe_3)_3(CO)Ru(SiMe_2CH_2CH_2SiMe_2H)H$ and 4% *mer*-$(PMe_3)_3(CO)Ru(SiMe_2CH_2CH_2SiMe_2H)H$.

*mer*-$(PMe_3)_3(CO)Ru(SiMe_2CH_2CH_2SiMe_2H)H$: $^1H$ NMR ($C_6D_6$) $\delta$ −9.05 (dt, $J_{PH}$ = 72 and 29 Hz, 1H, Ru*H*), 0.21 (d, $J_{HH}$ = 3.5 Hz, 6H, Si*Me*$_2$H), 0.42 (s, 6H, Si*Me*$_2$), 1.12 (d, $J_{PH}$ = 6 Hz, 9H, P*Me*$_3$), 1.28 (t, $J_{PH}$ = 3.0 Hz, 18H, mutually *trans*-P*Me*$_3$), 4.32 (m, 9 lines, $J_{HH}$ = 3.5 Hz, 1H, SiMe$_2$*H*). NB: The $CH_2$ resonances could not be reliably assigned. IR (petroleum ether) $\nu$(CO) = 1925 $cm^{-1}$.

*fac*-$(PMe_3)_3(CO)Ru(SiMe_2CH_2CH_2SiMe_2H)H$: $^1H$ NMR ($C_6D_6$) $\delta$ −9.11 (ddd $J_{PH}$ = 67.1, 29.7 and 21.8 Hz, 1H, Ru*H*), 0.22 (d, $J_{HH}$ = 3.5 Hz, 6H, Si*Me*$_2$H), 0.62 (d, $J_{PH}$ = 1.7 Hz, 3H, Si*Me*$_2$), 0.66 (d, $J_{PH}$ = 1 Hz, 2H, C*H*$_2$), 0.72 (d, $J_{PH}$ = 1.7 Hz, 3H, Si*Me*$_2$), 0.78 (s, 2H, C*H*$_2$), 1.07 (d, $J_{PH}$ = 7.0 Hz, 9H, P*Me*$_3$), 1.10 (d, $J_{PH}$ = 6.1 Hz, 9H, P*Me*$_3$), 1.11 (d, $J_{PH}$ = 6.1 Hz, 9H, P*Me*$_3$), 4.36 (m, 9 lines, $J_{HH}$ = 3.2 Hz, 1H, SiMe$_2$*H*); $^{31}P$ NMR ($C_6D_6$) $\delta$ −22.7 (dd, $J_{PH}$ = 21.5 and 36.8 Hz, 1P, *P*Me$_3$), −16.4 (m, 1P, *P*Me$_3$), −11.9 (t, $J_{PH}$ = 36.3 Hz, 1P, *P*Me$_3$), IR (petroleum ether) $\nu$(CO) = 1940 $cm^{-1}$.

**Generation of $(PMe_3)_3Ru(SiMe_3)_2(H)_2$ at Low Temperature.** Solid $[(PMe_3)_3Ru(H)(SiMe_3)_2]N_2$ (8 mg, 0.01 mmol) was loaded in an NMR tube assembly. Methylcyclohexane-$d_{14}$ (0.5 mL) was vacuum transferred into the tube. The sample was thawed out and kept at 0 °C for 30 s and at −10 °C for 5 min. It was then frozen and degassed. The freeze−pump−thaw cycle was repeated 4 times to remove most of ligated $N_2$ from $[(PMe_3)_3Ru(H)(SiMe_3)_2]N_2$ complex. $HSiMe_3$ was vacuum transferred into the tube (32.4 mL of vapor at 21 mmHg, 0.04 mmol) and the sample was flame sealed. It was thawed out at −78 °C and inserted in the pre-cooled (−125 °C) NMR probe.

$(PMe_3)_3Ru(SiMe_3)_2(H)_2$: $^1H$ NMR (methylcyclohexane-$d_{14}$, 148 K) $\delta$ −9.56 (br m, 1H, Ru*H*), −7.48 (br m, 1H, Ru*H*), 0.18 (br s, 9H, Si(C*H*$_3$)$_3$), 0.32 (br s, 9H, Si(C*H*$_3$)$_3$), 1.35 (br s, 27H, P*Me*$_3$); $^{31}P$ NMR (methylcyclohexane-$d_{14}$, 148 K) $\delta$ −13.7 (t, $J_{PH}$ = 37.5 Hz, 1P, *P*Me$_3$), −2.7 (d, $J_{PH}$ = 37.5 Hz, 2P, mutually *trans*-*P*Me$_3$).

**Reaction of $(PMe_3)_3Ru(SiMe_3)_2(H)_2$ with CO.** An NMR sample of $(PMe_3)_3Ru(SiMe_3)_2(H)_2$ in toluene-$d_8$ was prepared as described above. The mixture was stirred for 1 h at −78 °C. CO (7 equiv) were added, and the sample was flame sealed. It was thawed out at −78 °C and inserted in the pre-cooled (−100 °C) NMR probe. The only product at this temperature is *mer*-$(CO)(PMe_3)_3Ru(H)(SiMe_3)$, which subse-

quently isomerizes to the facial isomer upon warming to room temperature. Both compounds were identified by their $^1$H NMR, $^{31}$P NMR and IR spectra, as reported previously.[42]

**Single-Crystal X-ray Diffraction Analyses.** X-ray intensity data were collected on a Rigaku R-AXIS IIc area detector employing graphite-monochromated Mo Kα radiation ($\lambda = 0.710\ 69$ Å). Oscillation images were processed using bioteX,[74] producing a listing of unaveraged $F^2$ and $\sigma(F^2)$ values which were then passed to the teXsan[75] program package for further processing and structure solution on a Silicon Graphics Indigo R4000 computer.

For $(PMe_3)_3Ru(SiH_2Ph)_2(H)_2$ indexing was performed from a series of four 1° oscillations with exposures of 20 s per frame. A hemisphere of data was collected using 6° oscillations with exposures of 20 s per frame. A total of 20088 reflections were measured over the ranges: $4 \le 2\theta \le 54°$, $0 \le h \le 22$, $-20 \le k \le 20$, $-12 \le l \le 12$. The intensity data were corrected for Lorentz and polarization effects and an empirical absorption correction was applied.[76] Of the reflections measured, a total of 2553 unique reflections with $F^2 > 3\sigma(F^2)$ were used during subsequent structure refinement (244 parameters refined.) The structure was solved by direct methods (SIR88).[77] Refinement was by full-matrix least squares techniques based on $F$ to minimize the quantity $\sum w(|F_o| - |F_c|)^2$ with $w = 1/\sigma^2(F)$. Non-hydrogen atoms were refined anisotropically and hydrogen atoms were included as constant contributions to the structure factors and were not refined (hydrogens on Ru and Si could not be reliably located). The maximum $\Delta/\sigma$ in the final cycle of least squares was 0.077 and the two most prominent peaks in the final difference Fourier were +0.50 and −0.49 e/Å$^3$.

For $(PMe_3)_3Ru(SiMe_2CH_2CH_2SiMe_2)(H)_2$ indexing was performed from a series of 1° oscillation images with exposures of 200 s per frame. A hemisphere of data was collected using 5° oscillation angles with exposures of 150 s per frame and a crystal-to-detector distance of 70 mm. A total of 23 361 reflections were measured over the ranges $5.04 \le 2\theta \le 54.96°$, $-46 \le h \le 46$, $-12 \le k \le 12$, $-20 \le l \le 20$ yielding 5604 unique reflections ($R_{int} = 0.0337$). The intensity data were corrected for Lorentz and polarization effects but not for absorption. The structure was solved by Patterson methods (DIRDIF94).[78] Refinement was by full-matrix least squares based on $F^2$ using SHELXL-93.[79] A total of 371 parameters were refined, using all unique reflections. Reflections with $F^2$'s that were experimentally negative were set to zero. The weighting scheme used was $w = 1/[\sigma^2(F_o^2) + 0.0570P^2 + 11.1007P]$ where $P = (F_o^2 + 2F_c^2)/3$. Non-hydrogen atoms were refined anisotropically and hydrogen atoms were refined isotropically. The maximum $\Delta/\sigma$ in the final cycle of least squares was −0.002 and the two most prominent peaks in the final difference Fourier were +0.660 and −0.694 e/Å$^3$.

For $(PMe_3)_3Ru(SiMe_2CH_2SiMe_3)H_3$ indexing was performed from a series of 1° oscillation images with exposures of 50 s per frame. A hemisphere of data was collected using 5° oscillation angles with exposures of 150 s per frame and a crystal-to-detector distance of 82 mm. A total of 27 198 reflections were measured over the ranges $5.12 \le 2\theta \le 54.96°$, $-18 \le h \le 18$, $-24 \le k \le 24$, $-12 \le l \le 12$ yielding 5960 unique reflections ($R_{int} = 0.0297$). The intensity data were corrected for Lorentz and polarization effects and for absorption using REQAB4[80] (minimum and maximum transmission 0.781, 1.009). The structure was solved by direct methods (SIR92).[81] Refinement was by full-matrix least squares based on $F^2$ using SHELXL-93.[79] A total of 379 parameters were refined, using all unique reflections. Reflections with $F^2$'s that were experimentally negative were set to zero. The weighting scheme used was $w = 1/[\sigma^2(F_o^2) + 0.0678P^2 + 1.5991P]$ where $P = (F_o^2 + 2F_c^2)/3$. Non-hydrogen atoms were refined anisotropically and hydrogen atoms were refined isotropically. The maximum $\Delta/\sigma$ in the final cycle of least squares was 0.015 and the two most prominent peaks in the final difference Fourier were +0.783 and −0.649 e/Å$^3$.

**Acknowledgment.** We are grateful to the National Science Foundation (CHE-9904798) and Tokyo Electron Massachusetts for support of this work.

**Supporting Information Available:** X-ray crystallographic data for **3a**, **3c**, and **4b** in CIF format. This material is available free of charge via the Internet at http://pubs.acs.org.

JA035916V

(74) *bioteX: A Suite of Programs for the Collection, Reduction and Interpretation of Imaging Plate Data*; Molecular Structure Corporation, 1995.
(75) *teXsan: Crystal Structure Analysis Package*; Molecular Structure Corporation, 1985 and 1992.
(76) Miller, L. L.; Jacobson, R. A. *Computer Chem.* **1989**, *12*, 1.
(77) Burla, M. C.; Camalli, M.; Cascarano, G.; Giacovazzo, C.; Polidori, G.; Spagna, R.; Viterbo, D. *J. Appl. Crystallogr.* **1989**, *72*, 389−393.
(78) Beurskens, P. T.; Admiraal, G.; Beurskens, G.; Bosman, W. P.; de Gelder, R.; Israël, R.; Smits, J. M. M. *The DIRDIF-94 Program System*; Crystallography Laboratory, University of Nijmegen, The Netherlands, 1994.
(79) Sheldrick, G. M., *SHELXL-93: Program for the Refinement of Crystal Structures*; Göttingen University: Göttingen, Germany, 1993.
(80) Jacobsen, R. A. 1994, personal communication.
(81) SIR92: Altomare, A.; Burla, M. C.; Camalli, M.; Cascarano, M.; Giocovazzo, C.; Guagliardi, A.; Polidoro, G. *J. Appl. Crystallogr.* **1994**, *27*, 435.